Cell Reports

Article

# Optimal Maturation of the SIV-Specific CD8$^+$ T Cell Response after Primary Infection Is Associated with Natural Control of SIV: ANRS SIC Study

## Graphical Abstract

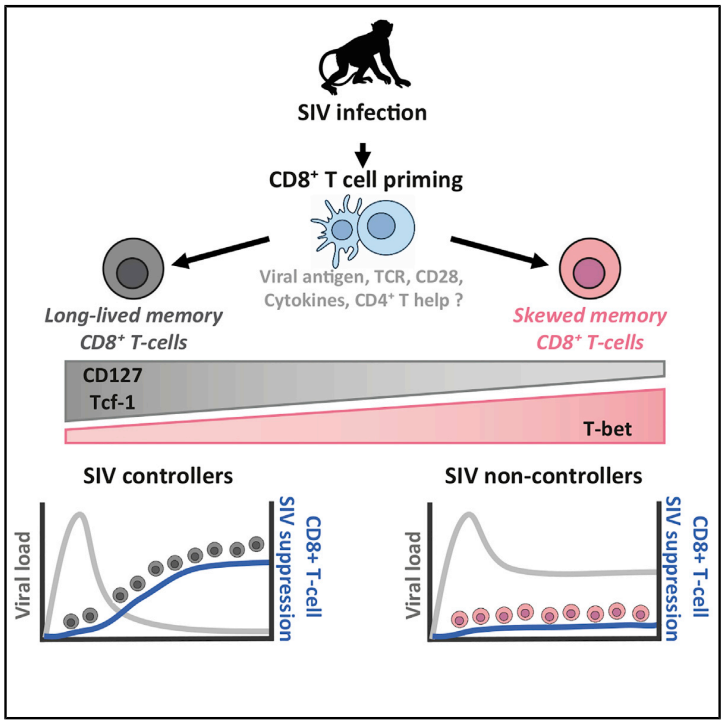


## Highlights

- SIV-specific CD8$^+$ T cells in acute infection show poor SIV-suppressive activity *ex vivo*
- SIV-suppressive activity increases over time in SIV controllers preceding viral control
- Controllers develop memory-like CD8$^+$ T cells, which seems to favor protective immunity
- Cells from non-controllers have a skewed phenotype and fail to gain antiviral potential

## Authors

Caroline Passaes, Antoine Millet, Vincent Madelain, ..., Véronique Avettand-Fenoel, Bruno Vaslin, Asier Sáez-Cirión

## Correspondence

bruno.vaslin@cea.fr (B.V.), asier.saez-cirion@pasteur.fr (A.S.-C.)

## In Brief

Using a cynomolgus macaque model of natural SIVmac251 control, Passaes et al. show that the capacity of SIV-specific CD8$^+$ T cells to suppress SIV is limited during acute infection but increases overtime in SIV controllers. This appears to be favored by the early establishment of optimal CD8$^+$ T cell memory.

Passaes et al., 2020, Cell Reports *32*, 108174
September 22, 2020 
https://doi.org/10.1016/j.celrep.2020.108174

CellPress

Cell Reports

CellPress
OPEN ACCESS

Article

# Optimal Maturation of the SIV-Specific CD8+ T Cell Response after Primary Infection Is Associated with Natural Control of SIV: ANRS SIC Study

Caroline Passaes,[1,2] Antoine Millet,[3] Vincent Madelain,[4] Valérie Monceaux,[1] Annie David,[1] Pierre Versmisse,[1] Naya Sylla,[2] Emma Gostick,[5] Sian Llewellyn-Lacey,[5] David A. Price,[5] Antoine Blancher,[6,7] Nathalie Dereuddre-Bosquet,[2] Delphine Desjardins,[2] Gianfranco Pancino,[1] Roger Le Grand,[2] Olivier Lambotte,[2,8] Michaela Müller-Trutwin,[1] Christine Rouzioux,[3,9] Jérémie Guedj,[4] Véronique Avettand-Fenoel,[3,9] Bruno Vaslin,[2,10,*] and Asier Sáez-Cirión[1,10,11,*]

[1]Institut Pasteur, HIV Inflammation and Persistence, Paris, France
[2]CEA-Université Paris-Saclay, INSERM UMR1184, Center for Immunology of Viral, Auto-immune, Hematologic and Bacterial Diseases, IDMIT Department, IBFJ, Fontenay-aux-Roses, France
[3]Université Paris-Descartes, Sorbonne Paris Cité, Faculté de Médecine, EA 7327 Paris, France
[4]Université Paris-Diderot, IAME, INSERM UMR 1137, Sorbonne Paris Cité, Paris, France
[5]Cardiff University School of Medicine, Division of Infection and Immunity, Cardiff, UK
[6]Université Paul Sabatier, Laboratoire d'Immunogénétique Moléculaire, EA 3034 Toulouse, France
[7]CHU de Toulouse, Laboratoire d'Immunologie, Toulouse, France
[8]Assistance Publique-Hôpitaux de Paris, Service de Médecine Interne et Immunologie Clinique, Groupe Hospitalier Université Paris-Saclay, Hôpital Bicêtre, Le Kremlin-Bicêtre, France
[9]Assistance Publique-Hôpitaux de Paris, Service de Microbiologie Clinique, Hôpital Necker-Enfants Malades, Paris, France
[10]These authors contributed equally
[11]Lead Contact
*Correspondence: bruno.vaslin@cea.fr (B.V.), asier.saez-cirion@pasteur.fr (A.S.-C.)
https://doi.org/10.1016/j.celrep.2020.108174

## SUMMARY

Highly efficient CD8+ T cells are associated with natural HIV control, but it has remained unclear how these cells are generated and maintained. We have used a macaque model of spontaneous SIVmac251 control to monitor the development of efficient CD8+ T cell responses. Our results show that SIV-specific CD8+ T cells emerge during primary infection in all animals. The ability of CD8+ T cells to suppress SIV is suboptimal in the acute phase but increases progressively in controller macaques before the establishment of sustained low-level viremia. Controller macaques develop optimal memory-like SIV-specific CD8+ T cells early after infection. In contrast, a persistently skewed differentiation phenotype characterizes memory SIV-specific CD8+ T cells in non-controller macaques. Accordingly, the phenotype of SIV-specific CD8+ T cells defined early after infection appears to favor the development of protective immunity in controllers, whereas SIV-specific CD8+ T cells in non-controllers fail to gain antiviral potency, feasibly as a consequence of early defects imprinted in the memory pool.

## INTRODUCTION

The ability of CD8+ T cells to control viral replication has been extensively documented in the setting of HIV/simian immunodeficiency virus (SIV) infection (McBrien et al., 2018; Walker and McMichael, 2012). Primary infection is characterized by massive viremia, which subsides following the expansion of HIV/SIV-specific CD8+ T cells (Borrow et al., 1994; Koup et al., 1994). However, the virus is not eradicated, leading to the emergence of immune escape variants (Allen et al., 2000; Borrow et al., 1997; O'Connor et al., 2002; Price et al., 1997) and ongoing antigen exposure, which drives CD8+ T cell exhaustion during the chronic phase of infection (Day et al., 2006; Petrovas et al., 2006, 2007; Trautmann et al., 2006). These observations suggest that naturally generated HIV/SIV-specific CD8+ T cells are frequently suboptimal in terms of antiviral efficacy, potentially reflecting limited cross-reactivity and/or intrinsic defects in the arsenal of effector functions required to eliminate infected CD4+ T cells (Du et al., 2016; Lécuroux et al., 2013). The latter possibility is especially intriguing in light of *ex vivo* experiments showing that effective suppression of viral replication is a particular feature of CD8+ T cells isolated from HIV controllers (HICs) (Angin et al., 2016; Sáez-Cirión et al., 2007, 2009; Tansiri et al., 2015).

HICs are a rare group of individuals who control viremia to low levels without antiretroviral therapy (Sáez-Cirión and Pancino, 2013). Understanding the mechanisms associated with such spontaneous control of HIV infection seems crucial for the development of new strategies designed to achieve remission. Efficient CD8+ T cell responses are almost universally present in

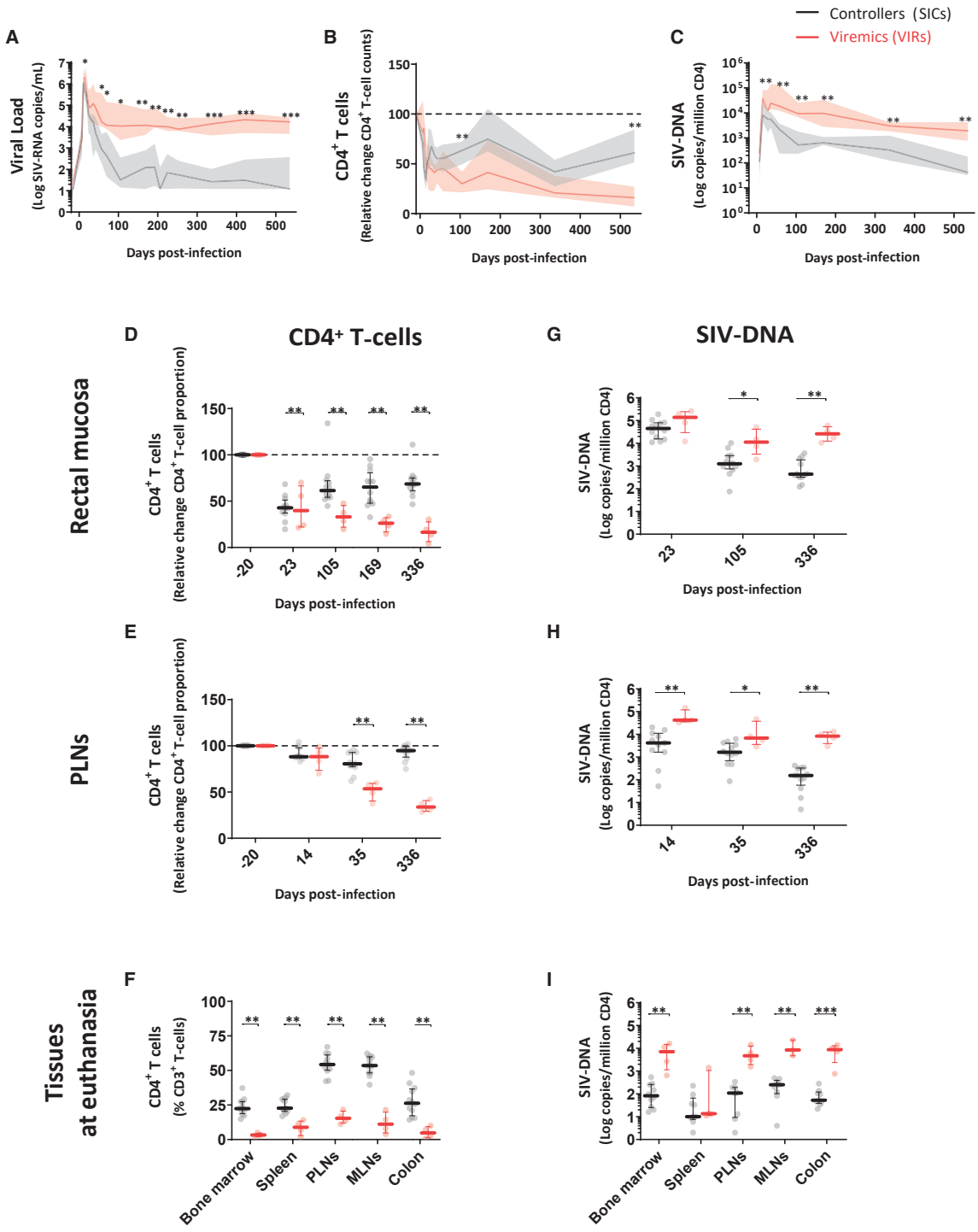


**Figure 1. SICs Are Characterized by Early Preservation of LNs and Progressive Decline in the Frequency of SIV-Carrying Cells**

(A–H) Plasma VL kinetics (A) and longitudinal evolution of CD4$^+$ T cell counts in blood (B), rectal mucosa (D), and PLNs (E) in SICs (gray) and VIRs (red). Results are shown as the fold change in absolute CD4$^+$ T cell counts relative to baseline in blood and as the fold change in the percentage of frequency of CD4$^+$ T cells among

*(legend continued on next page)*

HICs (Betts et al., 2006; Chowdhury et al., 2015; Hersperger et al., 2010, 2011a; Migueles et al., 2002, 2008; Sáez-Cirión et al., 2007, 2009; Zimmerli et al., 2005). These individuals also frequently express the protective human leukocyte antigen (HLA) class I allotypes HLA-B*27 or HLA-B*57, supporting a key role for $CD8^+$ T cells in the natural control of HIV (Lécuroux et al., 2014; Migueles et al., 2000; Pereyra et al., 2008). However, the presence of these allotypes is not sufficient to confer protection, and potent $CD8^+$ T cell responses with the ability to suppress HIV replication directly *ex vivo* also occur in HICs expressing non-protective allotypes (Lécuroux et al., 2014). In addition, the qualitative properties of $CD8^+$ T cells from HICs have only been characterized extensively during chronic infection, when viremia was already under control, often several years after the acquisition of HIV. It has therefore remained unclear how these high-quality $CD8^+$ T cell responses develop from the early stages of infection and evolve over time.

Cynomolgus macaques (CyMs, *Macaca fascicularis*) infected with SIVmac251 closely recapitulate the dynamics and key features of HIV infection, including similar levels of viral replication in the acute and chronic phases of infection, memory $CD4^+$ T cell depletion, rapid seeding of the viral reservoir, and eventual progression to AIDS (Antony and MacDonald, 2015; Feichtinger et al., 1990; Karlsson et al., 2007; Mannioui et al., 2009; Putkonen et al., 1989). Moreover, some individuals control infection naturally, as in humans. CyMs from Mauritius offer the additional advantage of limited major histocompatibility complex (MHC) diversity, making them particularly attractive for the study of $CD8^+$ T cell responses. Natural control of SIV in Mauritian CyMs is favored by the MHC haplotype M6 (Aarnink et al., 2011; Mee et al., 2009). Inoculation with low-dose SIV via the intrarectal (i.r.) route is also associated with natural control, irrespective of MHC haplotype (Bruel et al., 2015). We took advantage of these validated models to study the dynamics of SIV-specific $CD8^+$ T cell responses in blood and tissues from the onset of infection in controllers and viremic CyMs (VIRs). Using this approach, we identified an optimal maturation pathway in SICs that enabled SIV-specific $CD8^+$ T cells to acquire potent antiviral functions, which contributed to control of the infection.

## RESULTS

### SIV Controllers Are Characterized by Partial Restoration of $CD4^+$ T Cell Counts and Progressive Decline in the Frequency of SIV-Infected Cells in Blood

We monitored prospectively the outcome of infection in 12 SIV controllers (SICs) and 4 VIRs inoculated i.r. with SIVmac251. These animals carried or not the protective M6 haplotype and were inoculated with an animal infectious dose 50 ($AID_{50}$) of $5AID_{50}$ or $50AID_{50}$ of SIVmac251 (Table S1). SICs decreased plasma viral load (VL) to levels below 400 SIV-RNA copies/mL at least twice over a follow-up period of 18 months, whereas VIRs consistently maintained VL to levels above 400 SIV-RNA copies/mL. The threshold of 400 RNA copies/mL was chosen in coherence with our studies in human cohorts of natural HIV control (Angin et al., 2016; Noel et al., 2016; Sáez-Cirión et al., 2007, 2009, 2013). Ten SICs achieved control of viremia within 3 months. The other two SICs (BL669 and BO413) achieved VL below 400 SIV-RNA copies/mL for the first time 14 months after inoculation. One VIR (AV979) developed a tonsillar lymphoma, an AIDS-related event reported at high frequency in this species upon SIV infection (Feichtinger et al., 1990).

Some differences in peak viremia were observed between SICs and VIRs (Figure 1A; Table S2). These differences became more pronounced over time (Figure 1A), because plasma viremia was suppressed more rapidly in SICs versus VIRs (Table S2). Levels of cell-associated SIV-DNA in blood from SICs and VIRs were comparable before peak viremia, but differences became apparent as plasma VLs declined and were maintained throughout chronic infection (Figure 1C; Table S2). Likewise, $CD4^+$ T cells obtained during early infection from SICs and VIRs produced similar levels of p27 upon stimulation *ex vivo* with concanavalin A (ConA) and interleukin (IL) 2 (Figure S1A). However, although p27 production remained relatively stable in VIRs, these levels strongly dropped overtime in SICs. We found a significant correlation between the levels of p27 production by $CD4^+$ T cells and the levels of SIV-DNA ($r = 0.775$; $p = 0.0002$, 6 months post-infection [p.i.]). Therefore, our results show that SICs progressively reduced not only the frequency of total infected cells but also the translation-competent reservoir. In addition, $CD4^+$ T cell counts declined markedly in blood from both SICs and VIRs during primary infection (Figure 1B; Table S2). Subsequently, a degree of recovery was observed in SICs, whereas further gradual decline was observed in VIRs (Figure 1B; Table S2).

These results showed the distinctive dynamics of SIV infection in SICs and VIRs, characterized by modest differences during the early weeks following inoculation that were progressively exacerbated during transition to chronic infection. The differences between SICs and VIRs during the chronic phase of SIV infection were consistent with observations in human cohorts of HICs.

### SIV Control Is Associated with Early Preservation of Lymph Nodes

To characterize the extent of SIV control in greater depth, we monitored $CD4^+$ T cells and total SIV-DNA longitudinally in peripheral lymph nodes (PLNs) and rectal biopsies (RBs). At the end of the study, we conducted similar evaluations in bone marrow, spleen, mesenteric lymph nodes (MLNs), and colonic mucosa, comparing SICs versus VIRs. The frequency of $CD4^+$ T cells similarly declined in RBs from SICs and VIRs during the acute stage of primary infection. Although the frequency of $CD4^+$ T cells was later partially restored in SICs, it continued to decline in VIRs (Figure 1D). These results matched the observations in blood samples (Figure 1B). In contrast, the frequency of

$CD3^+$ lymphocytes relative to baseline in RBs and PLNs. (F) Percentage of frequency of $CD4^+$ T cells among $CD3^+$ lymphocytes in bone marrow, spleen, PLNs, MLNs, and colon mucosa at euthanasia. Kinetics of SIV-DNA levels in blood (C), RBs (G), and PLNs (H).

(I) Levels of SIV-DNA in bone marrow, spleen, PLNs, MLNs, and colon at euthanasia. Results are expressed as copies of SIV-DNA per million $CD4^+$ T cells. Median and interquartile range are shown (n = 12 SICs; n = 4 VIRs). *$p < 0.05$, **$p < 0.01$; Mann-Whitney U test.

$CD4^+$ T cells was maintained close to baseline in PLNs from SICs, even during primary infection (day 14 p.i.) but steadily declined over time in VIRs (Figure 1E). At the time of euthanasia, $CD4^+$ T cell frequencies were substantially higher in blood (Figure 1B), bone marrow, spleen, PLNs, MLNs, and colonic mucosa (Figure 1F) from SICs versus VIRs.

Cell-associated SIV-DNA levels closely mirrored the dynamics of $CD4^+$ T cells. Similarly high levels of cell-associated SIV-DNA were observed in RBs from SICs and VIRs during primary infection, but lower levels were observed in RBs from SICs versus VIRs during chronic infection (Figure 1G). SIV-DNA levels were already approximately 1 log lower in PLNs versus RBs from SICs during primary infection, and accordingly, lower levels were observed in PLNs from SICs versus VIRs since day 14 p.i. (Figure 1H). This finding suggests that early viral replication may be contained more efficiently in lymphoid nodes in SICs compared with other explored anatomical compartments. SIV-DNA was also detected in alveolar macrophages from all CyMs throughout the course of infection, again at lower levels in SICs versus VIRs during chronic infection (Figure S1B). In addition, SIV-DNA levels tended to decline progressively over time in SICs in all tissues analyzed, whereas SIV-DNA levels remained stable after primary infection in VIRs (Figures 1C, 1G, and 1H). At the time of euthanasia, SIV-DNA levels were substantially lower in blood (Figure 1C), bone marrow, PLNs, MLNs, and gut mucosa (Figure 1I; Figure S1C) from SICs versus VIRs.

Collectively, these data indicate that progressive systemic control of viral replication is achieved in SICs with $CD4^+$ T cell preservation and lower pan-anatomical reservoirs of SIV-DNA. Our results also underline the early preservation of PLNs in these animals.

## The Dynamics of $CD8^+$ T Cell Expansion and Activation Do Not Predict Control of SIV

To understand the mechanisms that contribute to immune control of SIV, we first monitored the proliferation and activation dynamics of total $CD8^+$ T cells in blood and lymphoid tissues from SICs and VIRs. Recent studies in hyperacute HIV-infected individuals indicate that the changes observed in total $CD8^+$ T cell activation during acute infection may be largely related to changes in the HIV-specific $CD8^+$ T cell pool (Ndhlovu et al., 2015; Takata et al., 2017). The frequencies of $CD8^+$ T cells expressing Ki-67 in blood increased to maximum levels during primary infection (measured peak at day 15 p.i.), coinciding with the measured peak of viremia, and then declined steadily to baseline levels during chronic infection (Figure 2A). Similar dynamics were observed in PLNs (Figure 2B) and gut mucosa (Figure 2C). In general, there were no significant differences between SICs and VIRs with respect to the dynamics of Ki-67 expression within the $CD8^+$ T cell pool, although lower frequencies of $CD8^+$ T cells expressing Ki-67 were observed during chronic infection in PLNs from SICs versus VIRs (Figure 2B).

The frequencies of $CD8^+$ T cells expressing the activation markers CD38 and HLA-DR in blood, PLNs, and gut mucosa increased similarly during primary infection (measured peak at day 28 p.i.), following the dynamics of Ki-67 expression in the same compartments (Figures 2D–2F). Again, there were no significant differences between SICs and VIRs with respect to the early dynamics of total $CD8^+$ T cell activation, but lower frequencies of $CD8^+$ T cells expressing CD38 and HLA-DR were observed during chronic infection in PLNs from SICs versus VIRs (Figure 2E).

Overall, our findings indicate that although lower activation and proliferation are observed in of $CD8^+$ T cells from SICs than from VIRs in the chronic stage of infection, the early proliferation and activation dynamics of the total pool of $CD8^+$ T cells do not distinguish subsequent progression rates.

## SIV-Specific $CD8^+$ T Cell Frequencies Do Not Predict Control of SIV

We analyzed $CD8^+$ T cell responses to a pool of optimal SIVmac251 peptides, which included peptides from different SIV proteins recognized by the most frequent MHC haplotypes in CyMs (M1, M2, and M3) and by the MHC haplotype M6 (Table S3). All animals carried at least one haplotype matching some peptide, and overall there was no difference in the number of tested peptides theoretically recognized in SICs and VIRs ($p = 0.35$). SIV-specific $CD8^+$ T cells producing tumor necrosis factor alpha (TNF-$\alpha$, the cytokine showing the lowest background in the absence of peptide or in presence of peptide during the baseline and hence used as reference) emerged in all CyMs during primary infection, coinciding with the peak of viremia, and no significant differences were observed between SICs and VIRs with respect to the frequencies of these cells in any anatomical compartment at any stage of infection (Figure 3A). Similarly, no consistent differences were observed between SICs and VIRs with respect to the frequencies of SIV-specific $CD8^+$ T cells that produced other cytokines, including interferon gamma (IFN$\gamma$) (Figure S2A) and IL-2 (Figure S2B), or mobilized CD107a (Figure S2C). The overall SIV-specific $CD8^+$ T cell response, determined in each CyM as the frequency of cells displaying at least one function (TNF-$\alpha$, IFN$\gamma$, IL-2, or CD107a), was also equivalent between SICs and VIRs across anatomical compartments throughout infection (Figure S2D). In addition, no clear differences between SICs and VIRs were observed with respect to the frequencies of SIV-specific $CD8^+$ T cells displaying at least three functions simultaneously in blood or PLNs during acute infection, but higher frequencies of polyfunctional SIV-specific $CD8^+$ T cells were present during chronic infection in lymphoid tissues from SICs versus VIRs (Figure 3B; Figure S2E). Differences also were not observed in the magnitude and polyfunction of SIV-specific $CD8^+$ T cells from SICs and VIRs when a pool of overlapping peptides spanning SIV Gag was used instead of the optimal peptide pool to stimulate the cells (Figure S3).

These data suggest that natural control of SIV is not associated with acutely generated, functionally superior SIV-specific $CD8^+$ T cell responses defined on the basis of cytokine production and degranulation.

## Progressive Acquisition of $CD8^+$ T Cell-Mediated SIV-Suppressive Activity Is Associated with Control of SIV

$CD8^+$ T cells from HICs typically suppress *ex vivo* infection of autologous $CD4^+$ T cells (Angin et al., 2016; Buckheit et al., 2012; Julg et al., 2010; Sáez-Cirión et al., 2007, 2009; Tansiri et al., 2015). We therefore investigated this property as a potential discriminant between SICs and VIRs. The capacity of $CD8^+$ T cells in blood and PLNs to suppress infection of autologous

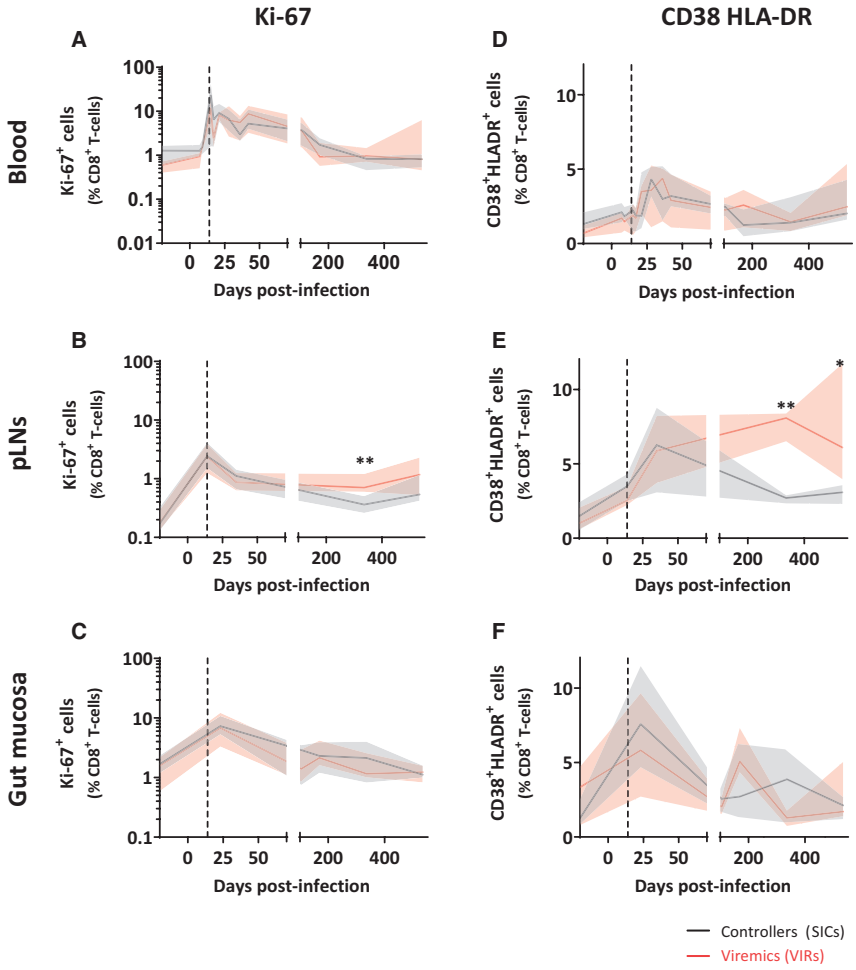


**Figure 2. The Dynamics of CD8+ T Cell Expansion and Activation Do Not Predict Control of SIV**

(A–C) Evolution of Ki-67+ CD8+ T cells in blood (A), PLNs (B), and rectal mucosa (C) in SICs (gray) and viremics (red).

(D–F) Evolution of CD38+ HLA-DR+ CD8+ T cells in blood (D), PLNs (E), and RB (F).

Median and interquartile range are shown. Vertical dashed lines indicate peak VLs. *p < 0.05, **p < 0.01; Mann-Whitney U test.

$CD4^+$ T cells was relatively weak in all CyMs during acute infection (Figure 4A), but this activity correlated negatively with VL on day 15 p.i. (Figure 4B, upper panel), suggesting its contribution to control viremia since early time points. Interestingly, the $CD8^+$ T cell-mediated SIV-suppressive activity increased substantially over time in SICs (Figure 4A; Figure S4A), either in blood or in tissues. No such acquisition of SIV-suppressive activity was observed in VIRs (Figure 4A; Figure S4A). Moreover, $CD8^+$ T cell-mediated SIV-suppressive activity on day 70 p.i. correlated negatively (or tended to correlate) with subsequent determinations of plasma VL (Figure S4B), and there was a negative correlation between the $CD8^+$ T cell-mediated SIV-suppressive activity at euthanasia and the VL at this time (Figure 4C, upper panels). In contrast, we never found negative correlations between VL (at any given time) and the suppressive capacity of $CD8^+$ T cells measured at subsequent time points. No significant correlations were identified at any time point between SIV-specific $CD8^+$ T cell frequencies, categorized according to TNF-$\alpha$ production in response to SIV peptides, and measurements of plasma VL (Figures 4B and 4C; Figure S4B, bottom panels). Moreover, $CD8^+$ T cell-mediated SIV-suppressive activity across the follow-up period, quantified as the area under the curve, tended to correlate negatively with plasma VL ($r_s = -0.47$, $p = 0.07$), whereas no such association was identified for the frequency of SIV-specific $CD8^+$ T cells ($r_s = -0.01$, $p = 0.97$) (Figure 4D). All these results indicate that changes in the suppressive capacity of $CD8^+$ T cell, but not in the frequency of SIV-specific $CD8^+$ T cells, were associated with SIV control. We have previously shown that strong HIV-suppressive capacity of $CD8^+$ T cells from HIV-1 controllers was linked to their ability to rapidly eliminate *ex vivo* autologous infected cells through cytotoxic mechanisms (Sáez-Cirión et al., 2007). Although we could not

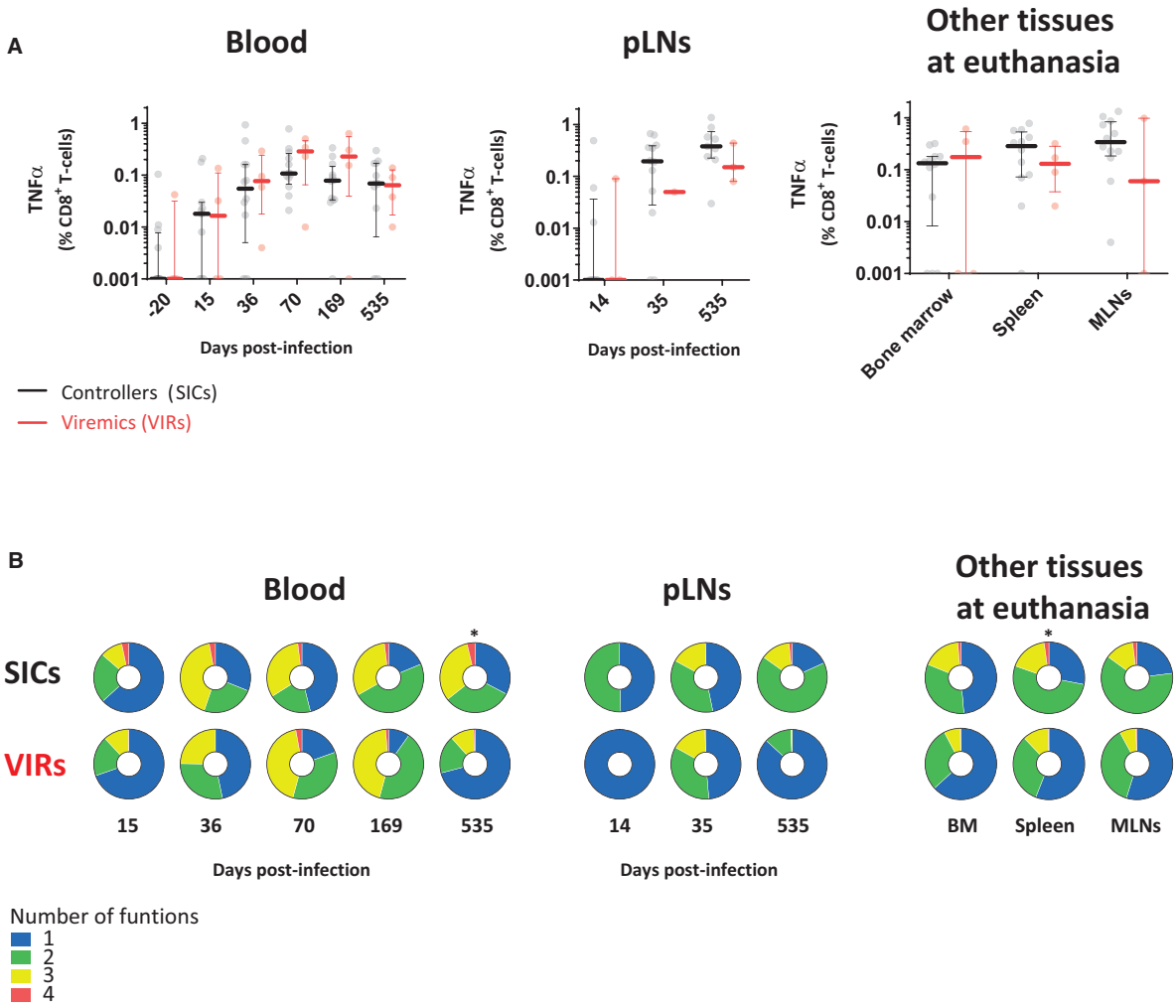


**Figure 3. SIV-Specific CD8⁺ T Cell Frequencies Do Not Predict Control of SIV**

(A) TNF-α production by SIV-specific CD8⁺ T cells in blood and PLNs over the course of infection and in bone marrow, spleen, and MLNs at euthanasia in SICs (gray) and VIRs (red). Results are shown as the percentage of frequency among CD8⁺ T cells. Median and interquartile range are shown (n = 12 SICs; n = 4 VIRs).

(B) Functional profiles of SIV-specific CD8⁺ T cells in blood and PLNs over the course of infection and in bone marrow, spleen, and MLNs at euthanasia. Doughnut charts show the median percentage of frequency of SIV-specific CD8⁺ T cells expressing IFNγ, TNF-α, IL-2, and/or CD107a (n = 12 SICs; n = 4 VIRs). Colors indicate number of simultaneous functions (blue, 1; green, 2; yellow, 3; red, 4).

*$p < 0.05$; Mann-Whitney U test.

repeat here all analyses we did in our studies in cohorts of HICs, we could confirm that the capacity of CD8⁺ T cells to suppress SIV infection *ex vivo* required contact with infected CD4⁺ T cells, and it was lost when CD8⁺ and CD4⁺ T cells were separated by transwell membranes (Figure S5A).

Our results exposed a disconnection between the development of SIV-specific CD8⁺ T cells responding to SIV peptides and the ability of these cells to suppress SIV infection, as measured in our viral inhibition assay *ex vivo* (Figure 4E; Figure S4A). SIV-specific CD8⁺ T cell frequencies increased sharply as the initial viremia began to fall and remained high for the duration of the study in CyMs, irrespective of their level of viremia. However, the substantial decline in viremia to levels below 400 copies/mL in SICs coincided with the rise of SIV-suppressive activity. The increase of CD8⁺ T cell-mediated SIV-suppressive activity was delayed in the late controllers BL669 and BO413, but nonetheless preceded optimal control of VL in these CyMs (Figure S4A). A strong capacity of CD8⁺ T cells to suppress SIV was observed at day 36 in the lymph nodes (LNs) from two animals (BA209 and BC657) that did not show such capacity in the blood (Figure 4A). Only one animal (29925) did not develop detectable SIV-suppressive activity during our follow-up. This animal had the weakest peak of viremia (1 log lower than any other) and achieved the fastest control (Figure S4A). Whether rapid or local

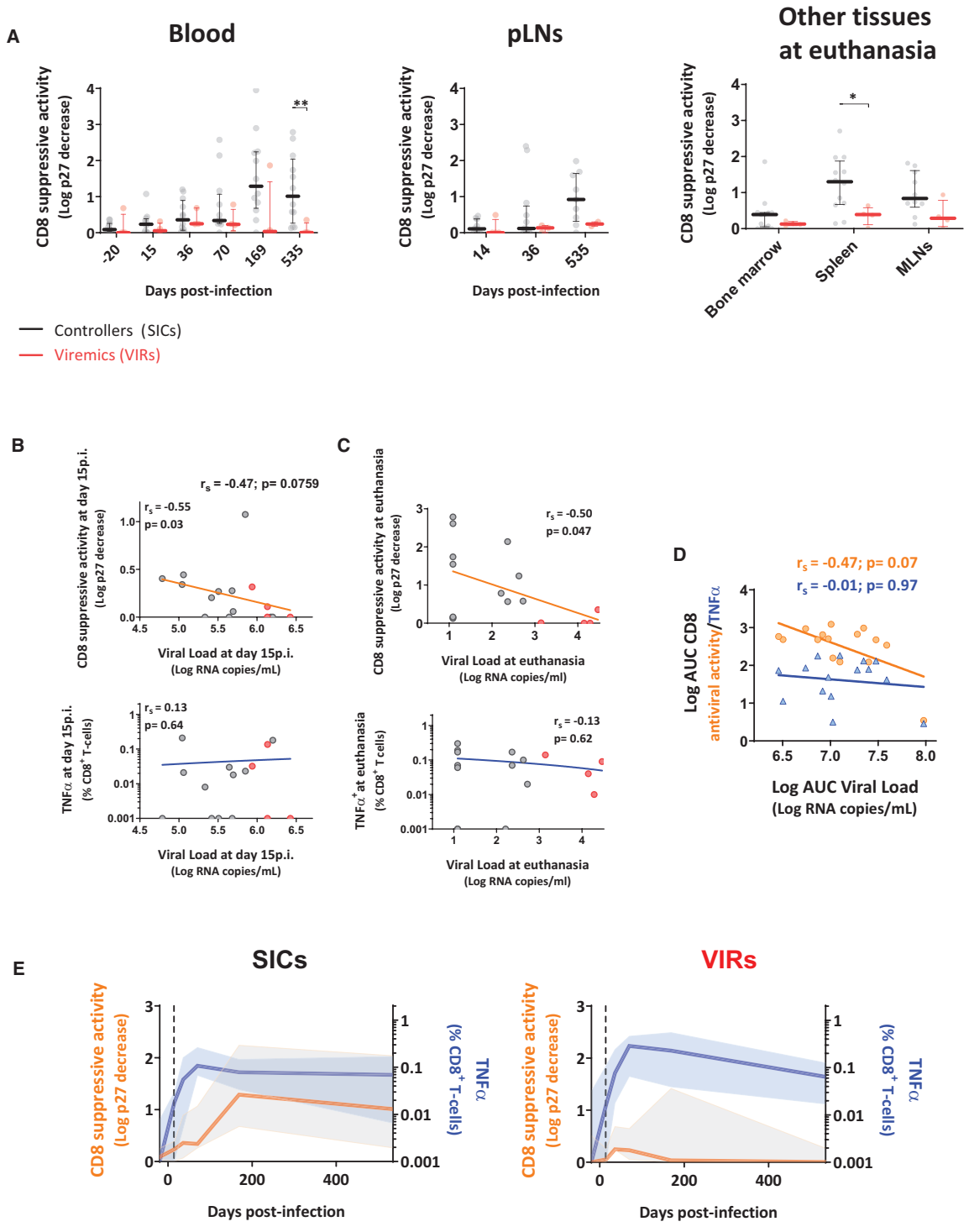


**Figure 4. Progressive Acquisition of CD8⁺ T Cell-Mediated SIV-Suppressive Activity Is Associated with Control of SIV**

(A) CD8⁺ T cell-mediated SIV-suppressive activity in blood and PLNs over the course of infection and in bone marrow, spleen, and MLNs at euthanasia in SICs (gray) and VIRs (red). Results are shown as the log p27 decrease in the presence of CD8⁺ T cells. *p < 0.05, **p < 0.01; Mann-Whitney U test.

*(legend continued on next page)*

development of the CD8$^+$ T cell suppressive capacity may have occurred or other mechanisms were associated with control of viremia in this animal remains unknown. At the time of euthanasia, superior CD8$^+$ T cell-mediated SIV-suppressive activity was detected in most SICs across all anatomical compartments, with the exception of bone marrow (Figure 4A), which nonetheless harbored SIV-specific CD8$^+$ T cells at frequencies comparable to those of other tissues (Figure 3A). Thus, although abundant, SIV-specific CD8$^+$ T cells induced during primary SIV infection had limited SIV-suppressive capacity when compared with cells found at later time points in SICs.

One limitation of our study was the reduced number of viremic animals we could compare in parallel to SICs. To confirm that the capacity of CD8$^+$ T cells to suppress *ex vivo* SIV infection did not increase in VIRs, we analyzed this activity in an additional group of 14 non-M6 CyMs infected intravenously (i.v.) with 1,000AID$_{50}$ of SIVmac251 and characterized by high-setpoint viremia (ANRS primate-viro-immunologic sustained control after treatment interruption [pVISCONTI] study). In these animals, the CD8$^+$ T cell-mediated SIV-suppressive activity remained modest throughout the follow-up (Figure S6A). The combined analysis of the CD8$^+$ T cells from all VIRs (n = 4 50AID$_{50}$ + n = 14 1,000AID$_{50}$) exposed early significant differences in the CD8$^+$ T cell-mediated SIV-suppressive activity when compared with the SICs ($p = 0.052$ at day 36 p.i. and $p < 0.05$ at days 70 and 169 p.i.; Figure S6B) and significantly higher capacity to suppress SIV infection of CD8$^+$ T cells from SICs than of cells from VIRs in all tissues analyzed at the end of the study (Figure S6B). Moreover, early initiation (day 28 p.i.) of antiretroviral treatment in another group of CyMs inoculated with 1,000AID$_{50}$ of SIVmac251 sharply decreased VL and CD8$^+$ T cell activation levels (Figure S6C) but did not change the capacity of CD8$^+$ T cells from these animals to suppress infection *ex vivo*, which remained extremely weak (Figure S6C). These results, which are in agreement with our previous observations in early-treated HIV-infected individuals (Lécuroux et al., 2013), show that low SIV-suppressive capacity during acute infection was a consequence neither of strong activation of these cells *in vivo* nor of high antigen burden.

Finally, one possible explanation for the weak SIV-suppressive capacity of CD8$^+$ T cells from VIRs was that they had limited capacity to recognize the SIVmac251 we used in our viral inhibition assay because of potential adaptation of the CD8$^+$ T cell response to evolving viruses in these CyMs. However, CD8$^+$ T cells from VIRs were not able to eliminate the CD4$^+$ T cells that produced autologous SIV upon activation *in vitro*. In contrast, although CD8$^+$ T cells from SICs were not able to suppress autologous virus during early infection, they acquired this capacity progressively at the same rate we found in our classical protocol (Figure S5B). These results confirmed that CD8$^+$ T cells from SICs and VIRs had functional differences that were unlinked to the evolution of the infecting virus.

Collectively, our results show that the capacity of SIV-specific CD8$^+$ T cells to suppress infection *ex vivo* was a genuine quality that progressively amplified in SICs. Our results further uncover a temporal link between acquisition by CD8$^+$ T cells of potent capacity to suppress infection and sustained control of SIV.

## Acquisition of CD8$^+$ T Cell-Mediated SIV-Suppressive Activity in SICs Occurs Independent of MHC Haplotype

Our primary intention in this study was to explore the mechanisms underlying natural control of SIV infection, independent of MHC background or infectious dose. However, as expected (Bruel et al., 2015), inoculation with low-dose virus and carriage of the protective M6 haplotype independently favored spontaneous control of viremia below 400 copies/mL in CyMs in our study (Figure S7A; Table S4). We therefore evaluated whether these parameters influenced the dynamics of control and the development of the CD8$^+$ T cell response upon infection. We found that CD4$^+$ T cells and the levels of cell-associated SIV-DNA similarly evolved in the blood and PLNs from M6 and non-M6 controllers (Figure S7B). There was a tendency for M6 controllers versus non-M6 controllers toward better recovery of CD4$^+$ T cells in blood at the end of the study ($p = 0.07$). Similarly, we did not find important differences between M6 and non-M6 controllers in their development of SIV-specific CD8$^+$ T cell responses (Figure S7C). M6 and non-M6 controllers developed similar frequencies of SIV-responding cells during acute infection that were maintained during follow-up. The capacity of CD8$^+$ T cells to suppress *ex vivo* SIV infection of CD4$^+$ T cells progressively increased in both M6 and non-M6 SICs. The only difference that we could appreciate was a faster acquisition (day 36 p.i.) of CD8$^+$ T cell-mediated SIV-suppressive activity in the PLNs from M6 SICs versus non-M6 SICs (Figure S7C). Intriguingly, non-M6 SICs had higher frequencies of SIV responding CD8$^+$ T cells in this tissue at the same time point. Overall, these results show that although the M6 background gave a selective advantage to CyMs to control infection in conditions of higher viral inoculum, this MHC haplotype was not indispensable for the acquisition of SIV-suppressive capacity by CD8$^+$ T cells, which occurred in both M6 and non-M6 SICs. The results are in agreement with the observations in HICs. Although cohorts of HICs are enriched in individuals carrying protective HLA class I alleles (mainly HLA-B*57 and HLA-B*27), many HICs do not carry protective HLA class I alleles but have CD8$^+$ T cells with strong

(B) Spearman correlations between CD8$^+$ T cell-mediated SIV-suppressive activity (upper panel) or TNF-$\alpha$ production by SIV-specific CD8$^+$ T cells (bottom panel) and plasma VL on day 15 p.i.

(C) Spearman correlations between CD8$^+$ T cell-mediated SIV-suppressive activity (upper panel) or TNF-$\alpha$ production by SIV-specific CD8$^+$ T cells (bottom panel) and plasma VL at euthanasia.

(D) Spearman correlations between area under the curve (AUC) for plasma VL and AUC for CD8$^+$ T cell-mediated SIV-suppressive activity (orange) and between AUC for plasma VL and AUC for TNF-$\alpha$ production by SIV-specific CD8$^+$ T cells (blue). AUC for plasma VL, TNF-$\alpha$ production, and CD8+ T cell antiviral activities were calculated using the sequential values obtained throughout the duration of our study in the blood of the infected animals (Figure S7).

(E) Side-by-side comparison of the longitudinal kinetics of TNF-$\alpha$ production by SIV-specific CD8$^+$ T cells in blood shown in Figure 2A (blue) and CD8$^+$ T cell-mediated SIV-suppressive activity in blood shown in Figure 3A (orange) in SICs (left panel) and VIRs (right panel). Median and interquartile range are shown (n = 12 SICs; n = 4 VIRs).

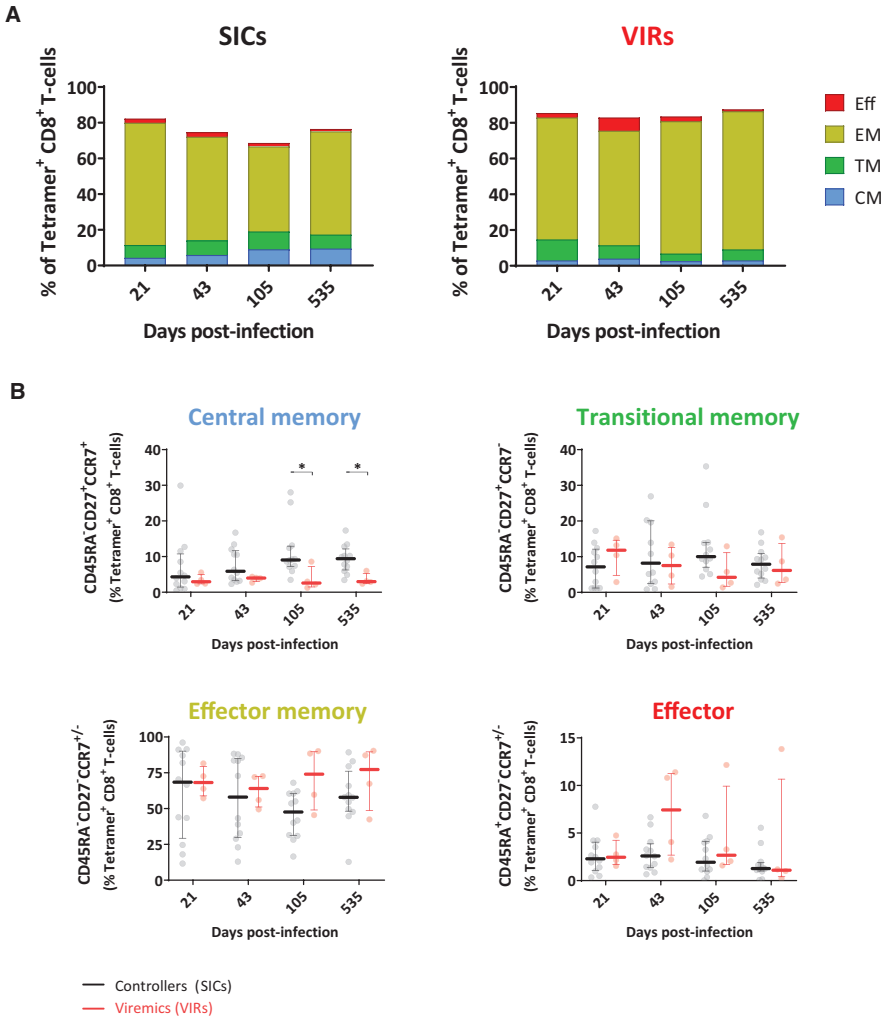


**Figure 5. SICs Maintain Higher Frequencies of SIV-Specific CM CD8$^+$ T Cells during Chronic Infection than VIRs**

(A) Bar charts showing the median percentage of frequency of SIV-specific CD8$^+$ T cells in each phenotypically defined subset in SICs and VIRs. Light blue, CM; green, TM; yellow, effector memory (EM); red, effector (Eff).

(B) Evolution of CM, TM, EM, and Eff SIV-specific CD8$^+$ T cells. Results are shown as the percentage of frequency of tetramer-binding CD8$^+$ T cells. Median and interquartile range are shown (n = 12 SICs; n = 4 VIRs). *p < 0.05; Mann-Whitney U test.

HIV-suppressive capacity *ex vivo* (Lécuroux et al., 2014). Therefore, the development of efficient CD8$^+$ T cell responses with antiviral activity is a characteristic of most HICs/SICs, independent of their MHC background.

## Skewed Maturation of Central Memory SIV-Specific CD8$^+$ T Cells Is Associated with Defective Acquisition of SIV-Suppressive Activity

To dissect the phenotypic correlates of antiviral potency measured *ex vivo*, we analyzed the differentiation status of SIV-specific CD8$^+$ T cells using selected markers in conjunction with MHC class I tetramers. Tetramer-binding SIV-specific CD8$^+$ T cells were detected in all CyMs and displayed early similar differentiation profiles in SICs and VIRs but evolved differently, such that higher frequencies of central memory (CM) SIV-specific CD8$^+$ T cells were present in SICs versus VIRs on day 105 p.i. ($p = 0.018$) and day 535 p.i. ($p = 0.013$) (Figures 5A and 5B).

In further analyses, we found that higher frequencies of SIV-specific CD8$^+$ T cells from SICs expressed the IL-7 receptor CD127, which is associated with cell survival and memory responses (Schluns et al., 2000), whereas higher frequencies of SIV-specific CD8$^+$ T cells from VIRs expressed the transcription factor T-bet, which is associated with cellular differentiation and effector functionality (Sullivan et al., 2003; Szabo et al., 2002) (Figure 6A). These differences seemed to appear since primary

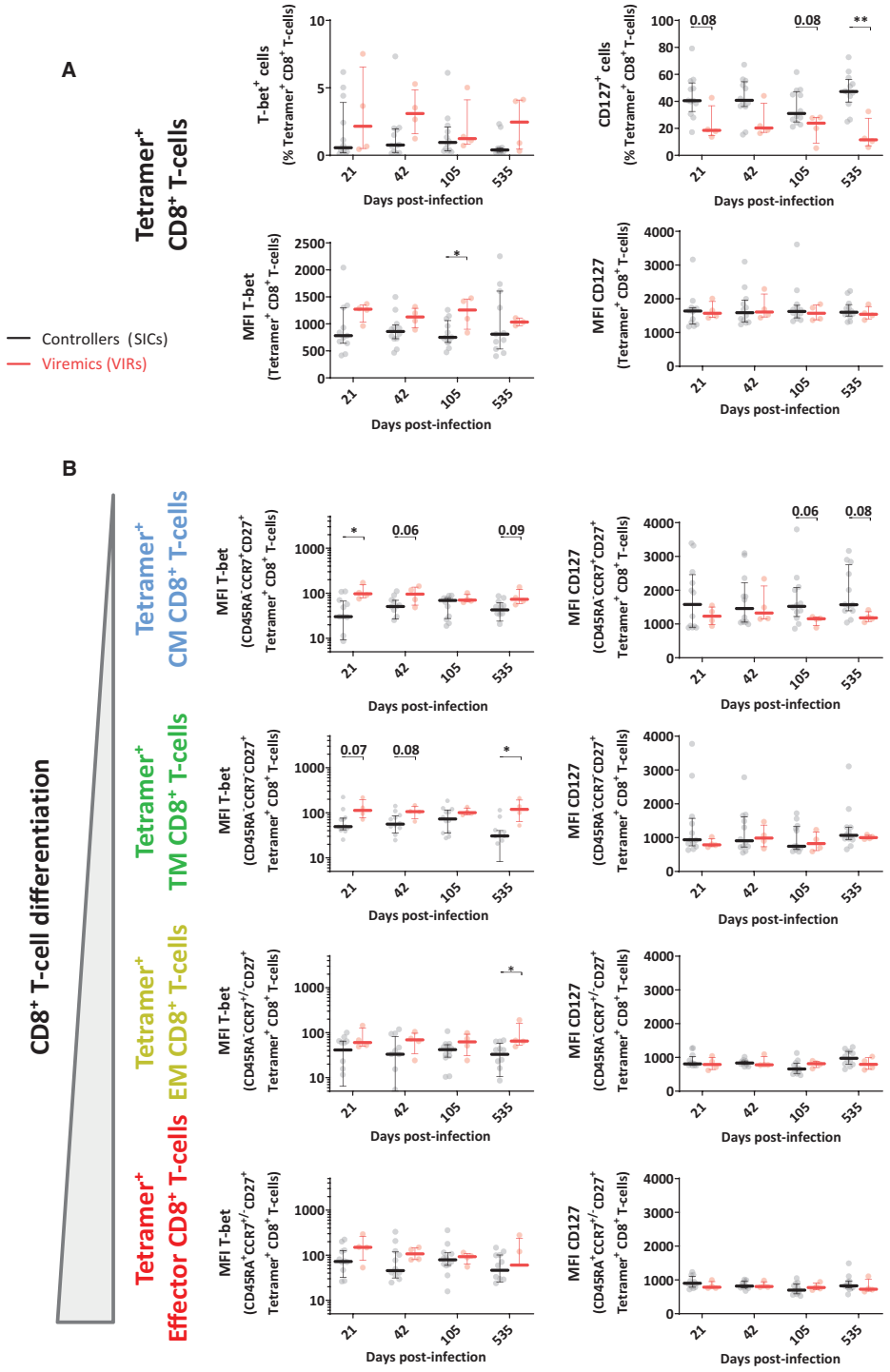


**Figure 6. Altered Maturation of CM SIV-Specific CD8⁺ T Cells in VIRs**

(A) Dynamics of T-bet expression (left panels) and CD127 expression (right panels) among SIV-specific CD8⁺ T cells in SICs (n = 12, gray) and VIRs (n = 4, red).

(B) Dynamics of T-bet expression (left) and CD127 expression (right) among CM, TM, EM, and Eff SIV-specific CD8⁺ T cells.

*p < 0.05, **p < 0.01; Mann-Whitney U test.

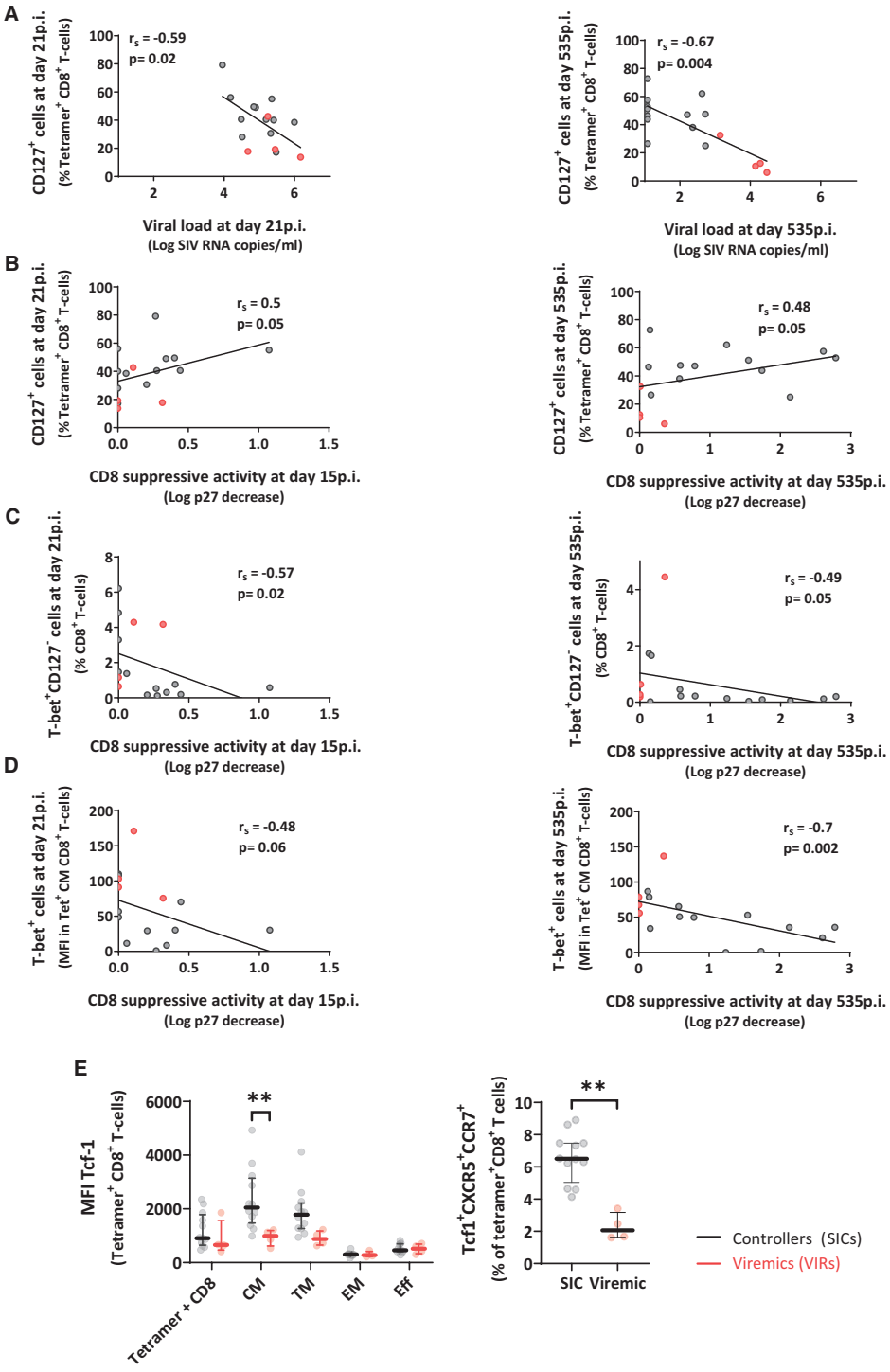


**Figure 7. Skewed Maturation of CM SIV-Specific CD8+ T Cells Is Associated with Defective Acquisition of SIV-Suppressive Activity**

(A and B) Spearman correlations between CD127+ SIV-specific CD8+ T cell frequencies and VLs (A) or CD8+ T cell-mediated SIV-suppressive activity (B) during acute infection (left panels) or chronic infection (right panels).

*(legend continued on next page)*

infection, but because of the limited number of VIRs analyzed, the differences only reached statistical significance at later time points (Figure 6A). Expression levels of CD127 and T-bet also varied as a function of differentiation among SIV-specific $CD8^+$ T cells from SICs and VIRs (Figure 6B). In particular, CM and transitional memory (TM) SIV-specific $CD8^+$ T cells expressed lower levels of T-bet throughout the course of infection in SICs versus VIRs, whereas CM SIV-specific $CD8^+$ T cells tended to express higher levels of CD127 during chronic infection in SICs versus VIRs.

To palliate the limited statistical power, we analyzed all animals together, taking into account the spectrum of outcomes rather than group classifications. We found negative correlations during primary infection and at euthanasia between the expression levels of CD127 on SIV-specific $CD8^+$ T cells and plasma VLs (Figure 7A). The levels of CD127 correlated positively with $CD8^+$ T cell-mediated SIV-suppressive activity at the same time points (Figure 7B). In contrast, negative correlations were observed during primary infection and at euthanasia between $CD8^+$ T cell-mediated SIV-suppressive activity and contemporaneous frequencies of T-$bet^+CD127^-$ SIV-specific $CD8^+$ T cells (Figure 7C) and between $CD8^+$ T cell-mediated SIV-suppressive activity and expression levels of T-bet among CM SIV-specific $CD8^+$ T cells (Figure 7D).

Altogether, these results point to the importance of the early establishment and maintenance of optimal memory $CD8^+$ T cell responses for achieving viral control. Recently, the presence of a population of memory-like $CD8^+$ T cells with stem-cell-like properties, characterized by the expression of the transcription factor T cell factor 1 (TCF-1) (Zhou et al., 2010), was shown to be critical to sustain the $CD8^+$ T cell response against chronic viral infections (Snell et al., 2018; Utzschneider et al., 2016). We found that SIV-specific CM $CD8^+$ T cells from SICs expressed higher levels of TCF-1 than cells from VIRs (Figure 7E). Among TCF-1-expressing cells, a higher frequency of cells from SICs also expressed CXCR5 and CCR7, revealing the presence of memory-like responses with the potential capacity to migrate to the LN follicles (Leong et al., 2016).

Collectively, these results suggest that SICs developed during early-infection SIV-specific $CD8^+$ T cells that enabled long-term memory potential, sustained antiviral activity, and viral control, whereas the corresponding SIV-specific $CD8^+$ T cells in VIRs adopt a skewed phenotype associated with cellular differentiation and suboptimal antiviral activity and were more prone to exhaustion (Zhou et al., 2010).

## DISCUSSION

This study provides insights into the immune correlates of natural SIV control. Although SIV-specific $CD8^+$ T cells were generated during acute infection with equivalent dynamics and global frequencies in all CyMs, preventing discrimination between SICs and VIRs, antiviral efficacy *ex vivo* developed progressively over time and was associated with spontaneous SIV control. This dichotomy was underpinned by distinct early-memory programs within the SIV-specific $CD8^+$ T cell pool. Collectively, these findings identify a cohesive set of immunological parameters that associate with effective and sustained control of SIV.

To monitor the establishment of natural control prospectively, we took advantage of previous reports showing that carriage of the MHC haplotype M6 and i.r. inoculation with low-dose ($5AID_{50}$) virus independently favor spontaneous control of SIVmac251 infection in CyMs (Aarnink et al., 2011; Bruel et al., 2015; Mee et al., 2009). Our results corroborate previous reports. In particular, although the presence of the M6 haplotype favored more frequent and more rapid control of infection among animals receiving a high dose of the virus ($50AID_{50}$) (Table S4), no significant differences were observed in the dynamics of SIV control in M6 and non-M6 SICs. At the time of euthanasia, a higher proportion of $CD4^+$ T cells and lower cell-associated SIV-DNA levels were found in multiple tissues from SICs versus VIRs, demonstrating systemic control of SIV. These differences were more subtle during primary infection. However, PLNs from SICs harbored approximately 10-fold less SIV-DNA in the acute phase than PLNs from VIRs. In addition, the frequency of $CD4^+$ T cells was maintained close to baseline throughout the course of the study in PLNs, but not in blood or RBs, from SICs. These observations suggest that early containment of viral replication in LNs (Buggert et al., 2018; Reuter et al., 2017) may be a key event for subsequent immune control of SIV.

In line with previous studies in humans (Lécuroux et al., 2013; Ndhlovu et al., 2015; Trautmann et al., 2012) and non-human primates (Veazey et al., 2001), we observed early and robust expansions of SIV-specific $CD8^+$ T cells in all CyMs. However, the functional profiles and overall frequencies of SIV-specific $CD8^+$ T cells (as determined by intracellular cytokine staining upon SIV antigen stimulation) during the acute phase of infection were largely equivalent in SICs and VIRs, and neither parameter correlated with subsequent determinations of plasma VL. Similarly, the functional profiles and overall frequencies of SIV-specific $CD8^+$ T cells during the chronic phase of infection were largely equivalent in SICs and VIRs, although polyfunctionality (defined as the capacity to simultaneously produce several cytokines and/or degranulate) was impaired at the time of euthanasia in VIRs. These results suggest that differences in polyfunctionality found during chronic infection are a surrogate marker of viral replication rather than an accurate determinant of antiviral efficacy, although the low number of animals in the VIR group may limit statistical power.

The capacity of $CD8^+$ T cells to suppress infection of autologous $CD4^+$ T cells directly *ex vivo* is a particular feature of HICs (Almeida et al., 2009; Angin et al., 2016; Buckheit et al.,

(C and D) Spearman correlations between T-$bet^+$ $CD127^-$ SIV-specific $CD8^+$ T cell frequencies (C) or T-bet expression levels in CM SIV-specific $CD8^+$ T cells (D) and $CD8^+$ T cell-mediated SIV-suppressive activity during acute infection (left panels) and chronic infection (right panels). Gray symbols, SICs (n = 12); red symbols, VIRs (n = 4).

(E) Expression levels of TCF-1 among total, CM, TM, EM, and Eff SIV-specific $CD8^+$ T cells (left panel) and proportion of SIV-specific $CD8^+$ T cells coexpressing TCF-1, CCR7, and CXCR5 (right panel). Median and interquartile range are shown.

$^{**}p < 0.01$; Mann-Whitney U test.

2012; Julg et al., 2010; Sáez-Cirión et al., 2007, 2009; Tansiri et al., 2015) that is mediated by the rapid elimination of infected CD4+ T cells through MHC-restricted mechanisms (Sáez-Cirión et al., 2007). Irrespective of subsequent outcome, we detected relatively weak $CD8^+$ T cell-mediated SIV-suppressive activity during primary infection, despite the vigorous mobilization of SIV-specific $CD8^+$ T cells. This observation parallels our previous findings in the setting of HIV (Lécuroux et al., 2013) and points to limited antiviral potential of $CD8^+$ T cell responses generated during primary infection. However, a negative correlation was already observed between $CD8^+$ T cell-mediated SIV-suppressive activity and viremia at this early time point, showing early temporal association of this antiviral activity and reduction of viremia. This SIV-suppressive capacity of $CD8^+$ T cells increased progressively over a period of weeks in some animals, carrying or not the protective MHC haplotype M6. At the time of euthanasia, these highly potent antiviral $CD8^+$ T cells were present in all tissues in SICs, with the exception of bone marrow, where this activity tended to be higher in SICs but overall weaker than in other tissues. $CD8^+$ T cell-mediated SIV suppression was also weak in PLNs during the first weeks following infection but increased over time in SICs. Therefore, the increase in the capacity of $CD8^+$ T cells to suppress infection was not the result of the recirculation of $CD8^+$ T cells from LNs once control was established but a genuine progressive augmentation of the antiviral potential of the cells. The development of potent antiviral $CD8^+$ T cells is therefore a *bone fide* correlate of sustained control of SIV.

We provide several arguments supporting that the progressive enhancement of the capacity of $CD8^+$ T cells to suppress SIV infection led to the establishment of controlled viremia, rather than evolving as a consequence of viral control. Because the dynamics of control were not homogeneous, we established a mathematical model to predict the development of effective immune-mediated control of SIV in our study (Madelain et al., 2020). Importantly, the model was constructed using SIV-RNA and SIV-DNA data exclusively from VIRs and SICs. SIV-RNA kinetics were best fitted using a model in which the cytotoxic immune response progressively mounted. The model predicted that faster decay in VL in SICs was associated with progressive development of a cytotoxic $CD8^+$ T cell response that decreased more than ten times the half-life of infected cells (from 5.5 days to 0.3 days). The model also predicted that in SICs, the maximal level of cytotoxic response was reached within 100 days of infection. The predictions of the kinetics of development of cytotoxic $CD8^+$ T cell responses matched, in *post hoc* analyses, the values of the capacity of $CD8^+$ T cells to suppress infection that we obtained experimentally, but not the frequency of $CD8^+$ T cells that responded to SIV peptides. Moreover, we found that SIV-suppressive activity of $CD8^+$ T cells 70 days after infection correlated negatively with ulterior VLs, although the suppressive activity never correlated negatively with preceding VLs. Control of viremia driven by antiretroviral treatment did not lead to the development of SIV-suppressive activity by $CD8^+$ T cells. Therefore, the enhancement of SIV-suppressive capacity does not occur in response to a decrease in antigen levels.

However, because of limited longitudinal sampling in lymphoid tissues, we cannot exclude that SIV control or emergence of SIV-suppressive capacity by $CD8^+$ T cells in these tissues preceded our observations. Moreover, the progressive establishment of control of infection and maturation of the $CD8^+$ T cell response might be the result of a virtuous circle, in which initial reduced dynamics of viral replication in LNs allowed the development of more effective $CD8^+$ T cell responses, which in turn droved a steeper reduction in viremia. "Goldilocks" levels of viral replication might then allow $CD8^+$ T cells to attain their maximal antiviral potential and sustain viral control, as has been proposed to occur in cytomegalovirus (CMV) infection (Picker, 2014).

$CD8^+$ T cells that can control certain latent chronic viral infections, such as CMV or Epstein-Barr virus (EBV), do not show features of functional exhaustion when compared with $CD8^+$ T cells against other chronic viral infections, such as SIV/HIV, hepatitis C virus (HCV), or hepatitis B virus (HBV) (Chatterjee et al., 2019; Fenwick et al., 2019; Luxenburger et al., 2018; van den Berg et al., 2019; Ye et al., 2015). This appears to be related to the development of $CD8^+$ T cells with distinct molecular programs that allow long-term memory and replenishment of the effector compartment in response to antigenic stimulation (Paley et al., 2012). Recent studies have identified a subset of memory-like $CD8^+$ T cells that express the transcription factor TCF-1 as responsible for sustaining the immune response against chronic viral infections (Utzschneider et al., 2016). $CD8^+$ T cells expressing TCF-1 have characteristics of CM cells, possess strong proliferative potential, and are able to produce a more differentiated cell subset while being less prone to exhaustion after repeated antigenic stimulation (Snell et al., 2018; Utzschneider et al., 2016; Zhou et al., 2010). We found that SIV-specific $CD8^+$ T cells from SICs expressed higher levels of TCF-1 than cells from VIRs, and these differences were more visible among less differentiated subsets and coupled with an enhanced expression of CXCR5, which may reflect the potential of these cells to migrate to germinal centers. During the revision of this manuscript, a preprint became available describing similar findings in cells from both HICs and SICs in an independent study (Rutishauser et al., 2020). In that study, the authors linked the expression of TCF-1 with the capacity of HIV-specific $CD8^+$ T cells to expand.

One decisive characteristic for the establishment of long-term memory is the capacity to upregulate the IL-7 receptor $\alpha$ subunit (CD127) (Huster et al., 2004). In addition, studies in mice have shown that decreased expression of T-bet among memory $CD8^+$ T cells allows the establishment of long-lived $CD127^{hi}$ cells, which maintain the capacity to proliferate and control successive infections (Joshi et al., 2007, 2011). In our study, the divergent outcome of SICs versus VIRs was preceded by early differences in the expression of CD127 and T-bet, especially within the less differentiated memory pool (CM and TM). In particular, at day 21 p.i., higher frequencies of SIV-specific CM $CD8^+$ T cells expressed CD127 in SICs, whereas higher frequencies of SIV-specific CM and TM $CD8^+$ T cells expressed T-bet in VIRs. Plasma viremia was uncontrolled at this time point and largely equivalent in animals that became SICs (median 5.19 log SIV-RNA) or VIRs (median 5.36, $p = 0.65$). The phenotypic differences remained consistent or even appeared to become more pronounced throughout the course of infection, although the statistical power of the analyses was affected by the limited number

of VIRs studied. Overall, our data suggest that SICs develop early-memory-like SIV-specific CD8$^+$ T cell responses, whereas VIRs develop SIV-specific memory CD8$^+$ T cell responses skewed toward more effector-like characteristics; they also suggest that these differences may be determinant to achieving and sustaining viral control. These findings are broadly consistent with several previous reports describing immune profiles that associate with the control of viremia in HICs during chronic infection. Favorable characteristics include high frequencies of CD57$^+$ eomesodermin$^{hi}$ HIV-specific CD8$^+$ T cells with superior proliferative capacity, increased expression levels of CD127, and intermediate expression levels of T-bet (Simonetta et al., 2014), as well as high frequencies of HIV-specific CD8$^+$ T cells with the capacity to upregulate T-bet, granzyme B, and perforin in response to antigen encounter (Hersperger et al., 2011b; Migueles et al., 2008).

In a single-cell study (Angin et al., 2019), we also found differences in the program of HIV-specific CM CD8$^+$ T cells from HICs and non-controllers. Although HIV-specific CM CD8$^+$ T cells from HICs upregulated the expression of effector genes linked with mTORC2 activation and cell survival (including CD127), CM cells from non-controllers had a skewed profile associated with mTORC1 activation (including T-bet) and glycolysis. This was traduced in a dependency on glucose of HIV-specific CD8$^+$ T cells from non-controllers to react to HIV antigens, whereas HIV-specific CD8$^+$ T cells from HICs were characterized by metabolic plasticity and were able to exert their function even in conditions of glucose deprivation. These differences in the metabolic program of cells from controllers and non-controllers could be recapitulated with SIV-specific CD8$^+$ T cells from SICs and VIR macaques from the present study (Angin et al., 2019), corroborating the validity of our CyM model to study the development of the protective CD8$^+$ T cell response characteristics of HICs and SICs. The present results extend these observations and support a key role for long-lived memory responses in the control of SIV. Importantly, our data also show that distinct memory responses are formed early after infection, potentially reflecting different priming conditions.

Several important questions remain unresolved. It remains unclear which factors are required to encourage the development of memory CD8$^+$ T cell responses that provide optimal protection against HIV/SIV. In some viral infections, expression of T-bet is tightly regulated by cytokines, such as IL-12 (Rao et al., 2012; Takemoto et al., 2006). A recent study in the lymphocytic choriomeningitis virus (LCMV) murine model of infection suggests that memory-like TCF-1 CD8$^+$ T cell responses with stemness potential and enhanced capacity to react upon secondary challenge are developed during early chronic infection (in an immunosuppressive environment), whereas memory cells that are developed at the onset of infection (in a pro-inflammatory environment) become short-term effectors and are rapidly exhausted (Snell et al., 2018). Based on these observations, we propose that balanced inflammatory responses (Barouch et al., 2016) arising as a consequence of lower viral burdens in the LNs during acute infection in SICs might facilitate antigen-specific priming events associated with optimal memory programs (Ozga et al., 2016) and minimize the loss of CD4$^+$ T cells, which provide helper functions that are critical for the development of long-lived memory-like CD8$^+$ T cells (Khanolkar et al., 2004; Utzschneider et al., 2016). However, it is unclear which mechanisms were responsible for the reduced viral dynamics in the LNs of SICs during acute infection. In the case of animals carrying the M6 haplotype, this could be related to more effective natural killer (NK) cell responses, as has been shown for humans carrying some protective HLA alleles (Martin et al., 2002). For animals inoculated with a lower dose of the virus, this could result from less diversity of infecting viruses (Liu et al., 2010), which could limit the inflammatory response and be more efficiently controlled by initial CD8$^+$ T cell responses. Although we have shown that the changes in the suppressive capacity of CD8$^+$ T cells were related to intrinsic functional properties of the cells, not to different capacities to react against evolving viruses, a better understanding of the evolution of viral diversity and the quality of immune responses appears important in light of our results. Finally, we found that the proportion of CD127$^+$ SIV-specific CD8$^+$ T cells during acute and chronic infection correlated positively with CD8$^+$ T cell-mediated SIV-suppressive activity, and we propose that the amplification of potent antiviral activity is the result of a maturation process, the trajectory of which is linked to the early optimal programming of the CD8$^+$ T cell memory compartment. However, we do not have direct evidence at the molecular level to explain why or how the capacity to suppress infection increased progressively among CD8$^+$ T cells. Maturation through persistent or repeated exposure to antigen can drive the selection of specific clonotypes bearing high-affinity T cell receptors (TCRs) (Busch and Pamer, 1999; Ozga et al., 2016; Price et al., 2005), which have been shown to suppress HIV replication more efficiently than clonotypes targeting the same antigen via low-affinity TCRs (Almeida et al., 2007, 2009; Ladell et al., 2013; Lima et al., 2020). Increase in antigen sensitivity over time would be compatible with the progressive increase in antiviral potency that we observed for the CD8$^+$ T cells from controllers in our study.

Collectively, the data presented here underscore the importance of early host-pathogen interactions in the development of adaptive immunity and reveal an optimal maturation pathway associated with the generation and maintenance of potent and sustained antiviral CD8$^+$ T cell responses, which in turn dictate the outcome of infection with SIV.

## STAR★METHODS

Detailed methods are provided in the online version of this paper and include the following:

- KEY RESOURCES TABLE
- RESOURCE AVAILABILITY
  - Lead Contact
  - Materials Availability
  - Data and Code Availability
- EXPERIMENTAL MODEL AND SUBJECT DETAILS
  - Ethical statement
  - Animals and SIV infection
- METHOD DETAILS
  - Blood collection and processing

## SUPPLEMENTAL INFORMATION

Supplemental Information can be found online at https://doi.org/10.1016/j.celrep.2020.108174.

## ACKNOWLEDGMENTS

This study was funded by the French National Agency for Research on AIDS and Viral Hepatitis (ANRS) and by MSDAvenir. Additional support was provided by the Programme Investissements d'Avenir (PIA), managed by the ANR under reference ANR-11-INBS-0008, funding Infectious Disease Models and Innovative Therapies (IDMIT, Fontenay-aux-Roses, France) infrastructure, and ANR-10-EQPX-02-01, funding the FlowCyTech Facility (IDMIT, Fontenay-aux-Roses, France). C.P. was supported by an ANRS postdoctoral fellowship, A.M. was supported by MSDAvenir, and D.A.P. was supported by a Wellcome Trust Senior Investigator Award. We thank Benoit Delache, Brice Targat, Claire Torres, Christelle Cassan, Jean-Marie Robert, Julie Morin, Patricia Brochard, Sabrina Guenounou, Sebastien Langlois, and Virgile Monnet for expert technical assistance; Antonio Cosma for helpful discussion; Lev Stimmer for anatomopathology expertise; Isabelle Mangeot-Méderlé for helpful project management at IDMIT; and Christophe Joubert for veterinarian assistance at the animal facility at CEA. The SIV1C cell line was provided by François Villinger. The SIVmac239 Gag Peptide Set was obtained through the NIH AIDS Reagent Program (Division of AIDS, NIAID, NIH). Emtricitabine (FTC), dolutegravir (DTG), and tenofovir disoproxil fumarate (TDF) were obtained from Gilead and ViiV Healthcare though the "IAS towards an HIV Cure" common material transfer agreement.

## AUTHOR CONTRIBUTIONS

C.P. and A.M. designed and performed experiments, analyzed data, and interpreted results. V. Madelain, J.G., and V.A.-F. analyzed data and interpreted results. V. Monceaux, A.D., P.V., and N.S. performed experiments and analyzed data. E.G., S.L.-L., and D.A.P. produced bespoke reagents. N.D.-B. and D.D. designed experiments, analyzed data, and interpreted results. D.A.P., A.B., G.P., R.L.G., O.L., M.M.-T., and C.R. interpreted results. B.V. and A.S.-C. designed experiments, analyzed data, interpreted results, and supervised the study. C.P., B.V., and A.S.-C. wrote the paper with assistance from A.M., V. Madelain, V. Monceaux, A.D., P.V., N.S., D.A.P., N.D.-B., R.L.G., O.L., M.M.-T., C.R., J.G., and V.A.-F.

## DECLARATION OF INTERESTS

The authors declare no competing interests.

Received: December 27, 2019
Revised: July 10, 2020
Accepted: August 28, 2020
Published: September 22, 2020

## REFERENCES

Aarnink, A., Dereuddre-Bosquet, N., Vaslin, B., Le Grand, R., Winterton, P., Apoil, P.A., and Blancher, A. (2011). Influence of the MHC genotype on the progression of experimental SIV infection in the Mauritian cynomolgus macaque. Immunogenetics *63*, 267–274.

Allen, T.M., O'Connor, D.H., Jing, P., Dzuris, J.L., Mothé, B.R., Vogel, T.U., Dunphy, E., Liebl, M.E., Emerson, C., Wilson, N., et al. (2000). Tat-specific cytotoxic T lymphocytes select for SIV escape variants during resolution of primary viraemia. Nature *407*, 386–390.

Almeida, J.R., Price, D.A., Papagno, L., Arkoub, Z.A., Sauce, D., Bornstein, E., Asher, T.E., Samri, A., Schnuriger, A., Theodorou, I., et al. (2007). Superior control of HIV-1 replication by CD8+ T cells is reflected by their avidity, polyfunctionality, and clonal turnover. J. Exp. Med. *204*, 2473–2485.

Almeida, J.R., Sauce, D., Price, D.A., Papagno, L., Shin, S.Y., Moris, A., Larsen, M., Pancino, G., Douek, D.C., Autran, B., et al. (2009). Antigen sensitivity is a major determinant of CD8+ T-cell polyfunctionality and HIV-suppressive activity. Blood *113*, 6351–6360.

Angin, M., Wong, G., Papagno, L., Versmisse, P., David, A., Bayard, C., Charmeteau-De Muylder, B., Besseghir, A., Thiébaut, R., Boufassa, F., et al.; ANRS CO5 IMMUNOVIR-2 Study Group (2016). Preservation of Lymphopoietic Potential and Virus Suppressive Capacity by CD8+ T Cells in HIV-2-Infected Controllers. J. Immunol. *197*, 2787–2795.

Angin, M., Volant, S., Passaes, C., Lecuroux, C., Monceaux, V., Dillies, M.-A., Valle-Casuso, J.C., Pancino, G., Vaslin, B., Le Grand, R., et al. (2019). Metabolic plasticity of HIV-specific CD8$^+$ T cells is associated with enhanced antiviral potential and natural control of HIV-1 infection. Nat. Metab. *1*, 704–716.

Antony, J.M., and MacDonald, K.S. (2015). A critical analysis of the cynomolgus macaque, *Macaca fascicularis*, as a model to test HIV-1/SIV vaccine efficacy. Vaccine *33*, 3073–3083.

Barouch, D.H., Ghneim, K., Bosche, W.J., Li, Y., Berkemeier, B., Hull, M., Bhattacharyya, S., Cameron, M., Liu, J., Smith, K., et al. (2016). Rapid Inflammasome Activation following Mucosal SIV Infection of Rhesus Monkeys. Cell *165*, 656–667.

Betts, M.R., Nason, M.C., West, S.M., De Rosa, S.C., Migueles, S.A., Abraham, J., Lederman, M.M., Benito, J.M., Goepfert, P.A., Connors, M., et al. (2006). HIV nonprogressors preferentially maintain highly functional HIV-specific CD8+ T cells. Blood *107*, 4781–4789.

Borrow, P., Lewicki, H., Hahn, B.H., Shaw, G.M., and Oldstone, M.B. (1994). Virus-specific CD8+ cytotoxic T-lymphocyte activity associated with control of viremia in primary human immunodeficiency virus type 1 infection. J. Virol. *68*, 6103–6110.

Borrow, P., Lewicki, H., Wei, X., Horwitz, M.S., Peffer, N., Meyers, H., Nelson, J.A., Gairin, J.E., Hahn, B.H., Oldstone, M.B., and Shaw, G.M. (1997). Antiviral pressure exerted by HIV-1-specific cytotoxic T lymphocytes (CTLs) during primary infection demonstrated by rapid selection of CTL escape virus. Nat. Med. *3*, 205–211.

Bruel, T., Hamimi, C., Dereuddre-Bosquet, N., Cosma, A., Shin, S.Y., Corneau, A., Versmisse, P., Karlsson, I., Malleret, B., Targat, B., et al. (2015). Long-term control of simian immunodeficiency virus (SIV) in cynomolgus macaques not associated with efficient SIV-specific CD8+ T-cell responses. J. Virol. *89*, 3542–3556.

Buckheit, R.W., 3rd, Salgado, M., Silciano, R.F., and Blankson, J.N. (2012). Inhibitory potential of subpopulations of CD8+ T cells in HIV-1-infected elite suppressors. J. Virol. *86*, 13679–13688.

Buggert, M., Nguyen, S., Salgado-Montes de Oca, G., Bengsch, B., Darko, S., Ransier, A., Roberts, E.R., Del Alcazar, D., Brody, I.B., Vella, L.A., et al. (2018). Identification and characterization of HIV-specific resident memory CD8$^+$ T cells in human lymphoid tissue. Sci. Immunol. *3*, eaar4526.

Busch, D.H., and Pamer, E.G. (1999). T cell affinity maturation by selective expansion during infection. J. Exp. Med. *189*, 701–710.

Carrington, M., Nelson, G.W., Martin, M.P., Kissner, T., Vlahov, D., Goedert, J.J., Kaslow, R., Buchbinder, S., Hoots, K., and O'Brien, S.J. (1999). HLA and HIV-1: heterozygote advantage and B*35-Cw*04 disadvantage. Science *283*, 1748–1752.

Chatterjee, B., Deng, Y., Holler, A., Nunez, N., Azzi, T., Vanoaica, L.D., Müller, A., Zdimerova, H., Antsiferova, O., Zbinden, A., et al. (2019). CD8+ T cells retain

protective functions despite sustained inhibitory receptor expression during Epstein-Barr virus infection *in vivo*. PLoS Pathog. *15*, e1007748.

Chowdhury, A., Hayes, T.L., Bosinger, S.E., Lawson, B.O., Vanderford, T., Schmitz, J.E., Paiardini, M., Betts, M., Chahroudi, A., Estes, J.D., and Silvestri, G. (2015). Differential Impact of *In Vivo* CD8+ T Lymphocyte Depletion in Controller versus Progressor Simian Immunodeficiency Virus-Infected Macaques. J. Virol. *89*, 8677–8686.

Day, C.L., Kaufmann, D.E., Kiepiela, P., Brown, J.A., Moodley, E.S., Reddy, S., Mackey, E.W., Miller, J.D., Leslie, A.J., DePierres, C., et al. (2006). PD-1 expression on HIV-specific T cells is associated with T-cell exhaustion and disease progression. Nature *443*, 350–354.

Du, V.Y., Bansal, A., Carlson, J., Salazar-Gonzalez, J.F., Salazar, M.G., Ladell, K., Gras, S., Josephs, T.M., Heath, S.L., Price, D.A., et al. (2016). HIV-1-Specific CD8 T Cells Exhibit Limited Cross-Reactivity during Acute Infection. J. Immunol. *196*, 3276–3286.

Feichtinger, H., Putkonen, P., Parravicini, C., Li, S.L., Kaaya, E.E., Böttiger, D., Biberfeld, G., and Biberfeld, P. (1990). Malignant lymphomas in cynomolgus monkeys infected with simian immunodeficiency virus. Am. J. Pathol. *137*, 1311–1315.

Fenwick, C., Joo, V., Jacquier, P., Noto, A., Banga, R., Perreau, M., and Pantaleo, G. (2019). T-cell exhaustion in HIV infection. Immunol. Rev. *292*, 149–163.

Hersperger, A.R., Pereyra, F., Nason, M., Demers, K., Sheth, P., Shin, L.Y., Kovacs, C.M., Rodriguez, B., Sieg, S.F., Teixeira-Johnson, L., et al. (2010). Perforin expression directly *ex vivo* by HIV-specific CD8 T-cells is a correlate of HIV elite control. PLoS Pathog. *6*, e1000917.

Hersperger, A.R., Martin, J.N., Shin, L.Y., Sheth, P.M., Kovacs, C.M., Cosma, G.L., Makedonas, G., Pereyra, F., Walker, B.D., Kaul, R., et al. (2011a). Increased HIV-specific CD8+ T-cell cytotoxic potential in HIV elite controllers is associated with T-bet expression. Blood *117*, 3799–3808.

Hersperger, A.R., Migueles, S.A., Betts, M.R., and Connors, M. (2011b). Qualitative features of the HIV-specific CD8+ T-cell response associated with immunologic control. Curr. Opin. HIV AIDS *6*, 169–173.

Huster, K.M., Busch, V., Schiemann, M., Linkemann, K., Kerksiek, K.M., Wagner, H., and Busch, D.H. (2004). Selective expression of IL-7 receptor on memory T cells identifies early CD40L-dependent generation of distinct CD8+ memory T cell subsets. Proc. Natl. Acad. Sci. USA *101*, 5610–5615.

Joshi, N.S., Cui, W., Chandele, A., Lee, H.K., Urso, D.R., Hagman, J., Gapin, L., and Kaech, S.M. (2007). Inflammation directs memory precursor and short-lived effector CD8(+) T cell fates via the graded expression of T-bet transcription factor. Immunity *27*, 281–295.

Joshi, N.S., Cui, W., Dominguez, C.X., Chen, J.H., Hand, T.W., and Kaech, S.M. (2011). Increased numbers of preexisting memory CD8 T cells and decreased T-bet expression can restrain terminal differentiation of secondary effector and memory CD8 T cells. J. Immunol. *187*, 4068–4076.

Julg, B., Williams, K.L., Reddy, S., Bishop, K., Qi, Y., Carrington, M., Goulder, P.J., Ndung'u, T., and Walker, B.D. (2010). Enhanced anti-HIV functional activity associated with Gag-specific CD8 T-cell responses. J. Virol. *84*, 5540–5549.

Karlsson, I., Malleret, B., Brochard, P., Delache, B., Calvo, J., Le Grand, R., and Vaslin, B. (2007). Dynamics of T-cell responses and memory T cells during primary simian immunodeficiency virus infection in cynomolgus macaques. J. Virol. *81*, 13456–13468.

Khanolkar, A., Fuller, M.J., and Zajac, A.J. (2004). CD4 T cell-dependent CD8 T cell maturation. J. Immunol. *172*, 2834–2844.

Koup, R.A., Safrit, J.T., Cao, Y., Andrews, C.A., McLeod, G., Borkowsky, W., Farthing, C., and Ho, D.D. (1994). Temporal association of cellular immune responses with the initial control of viremia in primary human immunodeficiency virus type 1 syndrome. J. Virol. *68*, 4650–4655.

Ladell, K., Hashimoto, M., Iglesias, M.C., Wilmann, P.G., McLaren, J.E., Gras, S., Chikata, T., Kuse, N., Fastenackels, S., Gostick, E., et al. (2013). A molecular basis for the control of preimmune escape variants by HIV-specific CD8+ T cells. Immunity *38*, 425–436.

Lécuroux, C., Girault, I., Chéret, A., Versmisse, P., Nembot, G., Meyer, L., Rouzioux, C., Pancino, G., Venet, A., and Sáez-Cirión, A.; ANRS 147 OPTIPRIM clinical trial (2013). CD8 T-cells from most HIV-infected patients lack *ex vivo* HIV-suppressive capacity during acute and early infection. PLoS ONE *8*, e59767.

Lécuroux, C., Sáez-Cirión, A., Girault, I., Versmisse, P., Boufassa, F., Avettand-Fenoël, V., Rouzioux, C., Meyer, L., Pancino, G., Lambotte, O., et al. (2014). Both HLA-B*57 and plasma HIV RNA levels contribute to the HIV-specific CD8+ T cell response in HIV controllers. J. Virol. *88*, 176–187.

Leong, Y.A., Chen, Y., Ong, H.S., Wu, D., Man, K., Deleage, C., Minnich, M., Meckiff, B.J., Wei, Y., Hou, Z., et al. (2016). CXCR5(+) follicular cytotoxic T cells control viral infection in B cell follicles. Nat. Immunol. *17*, 1187–1196.

Lima, N.S., Takata, H., Huang, S.H., Haregot, A., Mitchell, J., Blackmore, S., Garland, A., Sy, A., Cartwright, P., Routy, J.P., et al. (2020). CTL Clonotypes with Higher TCR Affinity Have Better Ability to Reduce the HIV Latent Reservoir. J. Immunol. *205*, 699–707.

Liu, J., Keele, B.F., Li, H., Keating, S., Norris, P.J., Carville, A., Mansfield, K.G., Tomaras, G.D., Haynes, B.F., Kolodkin-Gal, D., et al. (2010). Low-dose mucosal simian immunodeficiency virus infection restricts early replication kinetics and transmitted virus variants in rhesus monkeys. J. Virol. *84*, 10406–10412.

Luxenburger, H., Neumann-Haefelin, C., Thimme, R., and Boettler, T. (2018). HCV-Specific T Cell Responses During and After Chronic HCV Infection. Viruses *10*, 645.

Madelain, V., Passaes, C., Millet, A., Avettand-Fenoel, V., Djidjou-Demasse, R., Dereuddre-Bosquet, N., Le Grand, R., Rouzioux, C., Vaslin, B., Saez-Cirion, A., et al. (2020). Modeling SIV kinetics supports that cytotoxic response drives natural control and unravels heterogeneous populations of infected cells. bioRxiv. https://doi.org/10.1101/2020.01.19.911594.

Mannioui, A., Bourry, O., Sellier, P., Delache, B., Brochard, P., Andrieu, T., Vaslin, B., Karlsson, I., Roques, P., and Le Grand, R. (2009). Dynamics of viral replication in blood and lymphoid tissues during SIVmac251 infection of macaques. Retrovirology *6*, 106.

Martin, M.P., Gao, X., Lee, J.H., Nelson, G.W., Detels, R., Goedert, J.J., Buchbinder, S., Hoots, K., Vlahov, D., Trowsdale, J., et al. (2002). Epistatic interaction between KIR3DS1 and HLA-B delays the progression to AIDS. Nat. Genet. *31*, 429–434.

McBrien, J.B., Kumar, N.A., and Silvestri, G. (2018). Mechanisms of CD8$^+$ T cell-mediated suppression of HIV/SIV replication. Eur. J. Immunol. *48*, 898–914.

Mee, E.T., Berry, N., Ham, C., Sauermann, U., Maggiorella, M.T., Martinon, F., Verschoor, E.J., Heeney, J.L., Le Grand, R., Titti, F., et al. (2009). Mhc haplotype H6 is associated with sustained control of SIVmac251 infection in Mauritian cynomolgus macaques. Immunogenetics *61*, 327–339.

Migueles, S.A., Sabbaghian, M.S., Shupert, W.L., Bettinotti, M.P., Marincola, F.M., Martino, L., Hallahan, C.W., Selig, S.M., Schwartz, D., Sullivan, J., and Connors, M. (2000). HLA B*5701 is highly associated with restriction of virus replication in a subgroup of HIV-infected long term nonprogressors. Proc. Natl. Acad. Sci. USA *97*, 2709–2714.

Migueles, S.A., Laborico, A.C., Shupert, W.L., Sabbaghian, M.S., Rabin, R., Hallahan, C.W., Van Baarle, D., Kostense, S., Miedema, F., McLaughlin, M., et al. (2002). HIV-specific CD8+ T cell proliferation is coupled to perforin expression and is maintained in nonprogressors. Nat. Immunol. *3*, 1061–1068.

Migueles, S.A., Osborne, C.M., Royce, C., Compton, A.A., Joshi, R.P., Weeks, K.A., Rood, J.E., Berkley, A.M., Sacha, J.B., Cogliano-Shutta, N.A., et al. (2008). Lytic granule loading of CD8+ T cells is required for HIV-infected cell elimination associated with immune control. Immunity *29*, 1009–1021.

Ndhlovu, Z.M., Kamya, P., Mewalal, N., Kløverpris, H.N., Nkosi, T., Pretorius, K., Laher, F., Ogunshola, F., Chopera, D., Shekhar, K., et al. (2015). Magnitude and Kinetics of CD8+ T Cell Activation during Hyperacute HIV Infection Impact Viral Set Point. Immunity *43*, 591–604.

Noel, N., Peña, R., David, A., Avettand-Fenoel, V., Erkizia, I., Jimenez, E., Lecuroux, C., Rouzioux, C., Boufassa, F., Pancino, G., et al. (2016). Long-Term

Spontaneous Control of HIV-1 Is Related to Low Frequency of Infected Cells and Inefficient Viral Reactivation. J. Virol. *90*, 6148–6158.

O'Connor, D.H., Allen, T.M., Vogel, T.U., Jing, P., DeSouza, I.P., Dodds, E., Dunphy, E.J., Melsaether, C., Mothé, B., Yamamoto, H., et al. (2002). Acute phase cytotoxic T lymphocyte escape is a hallmark of simian immunodeficiency virus infection. Nat. Med. *8*, 493–499.

O'Connor, S.L., Lhost, J.J., Becker, E.A., Detmer, A.M., Johnson, R.C., Macnair, C.E., Wiseman, R.W., Karl, J.A., Greene, J.M., Burwitz, B.J., et al. (2010). MHC heterozygote advantage in simian immunodeficiency virus-infected Mauritian cynomolgus macaques. Sci. Transl. Med. *2*, 22ra18.

Ozga, A.J., Moalli, F., Abe, J., Swoger, J., Sharpe, J., Zehn, D., Kreutzfeldt, M., Merkler, D., Ripoll, J., and Stein, J.V. (2016). pMHC affinity controls duration of CD8+ T cell-DC interactions and imprints timing of effector differentiation versus expansion. J. Exp. Med. *213*, 2811–2829.

Paley, M.A., Kroy, D.C., Odorizzi, P.M., Johnnidis, J.B., Dolfi, D.V., Barnett, B.E., Bikoff, E.K., Robertson, E.J., Lauer, G.M., Reiner, S.L., and Wherry, E.J. (2012). Progenitor and terminal subsets of CD8+ T cells cooperate to contain chronic viral infection. Science *338*, 1220–1225.

Pereyra, F., Addo, M.M., Kaufmann, D.E., Liu, Y., Miura, T., Rathod, A., Baker, B., Trocha, A., Rosenberg, R., Mackey, E., et al. (2008). Genetic and immunologic heterogeneity among persons who control HIV infection in the absence of therapy. J. Infect. Dis. *197*, 563–571.

Petrovas, C., Casazza, J.P., Brenchley, J.M., Price, D.A., Gostick, E., Adams, W.C., Precopio, M.L., Schacker, T., Roederer, M., Douek, D.C., and Koup, R.A. (2006). PD-1 is a regulator of virus-specific CD8+ T cell survival in HIV infection. J. Exp. Med. *203*, 2281–2292.

Petrovas, C., Price, D.A., Mattapallil, J., Ambrozak, D.R., Geldmacher, C., Cecchinato, V., Vaccari, M., Tryniszewska, E., Gostick, E., Roederer, M., et al. (2007). SIV-specific CD8+ T cells express high levels of PD1 and cytokines but have impaired proliferative capacity in acute and chronic SIVmac251 infection. Blood *110*, 928–936.

Picker, L.J. (2014). Are effector memory T cells the key to an effective HIV/AIDS vaccine? EMBO Rep. *15*, 820–821.

Price, D.A., Goulder, P.J., Klenerman, P., Sewell, A.K., Easterbrook, P.J., Troop, M., Bangham, C.R., and Phillips, R.E. (1997). Positive selection of HIV-1 cytotoxic T lymphocyte escape variants during primary infection. Proc. Natl. Acad. Sci. USA *94*, 1890–1895.

Price, D.A., Brenchley, J.M., Ruff, L.E., Betts, M.R., Hill, B.J., Roederer, M., Koup, R.A., Migueles, S.A., Gostick, E., Wooldridge, L., et al. (2005). Avidity for antigen shapes clonal dominance in CD8+ T cell populations specific for persistent DNA viruses. J. Exp. Med. *202*, 1349–1361.

Putkonen, P., Warstedt, K., Thorstensson, R., Benthin, R., Albert, J., Lundgren, B., Oberg, B., Norrby, E., and Biberfeld, G. (1989). Experimental infection of cynomolgus monkeys (*Macaca fascicularis*) with simian immunodeficiency virus (SIVsm). J. Acquir. Immune Defic. Syndr. *2*, 359–365.

Rao, R.R., Li, Q., Gubbels Bupp, M.R., and Shrikant, P.A. (2012). Transcription factor Foxo1 represses T-bet-mediated effector functions and promotes memory CD8(+) T cell differentiation. Immunity *36*, 374–387.

Reuter, M.A., Del Rio Estrada, P.M., Buggert, M., Petrovas, C., Ferrando-Martinez, S., Nguyen, S., Sada Japp, A., Ablanedo-Terrazas, Y., Rivero-Arrieta, A., Kuri-Cervantes, L., et al. (2017). HIV-Specific $CD8^+$ T Cells Exhibit Reduced and Differentially Regulated Cytolytic Activity in Lymphoid Tissue. Cell Rep. *21*, 3458–3470.

Rutishauser, R.L., Deguit, C.D.T., Hiatt, J., Blaeschke, F., Roth, T.L., Wang, L., Raymond, K., Starke, C.E., Mudd, J.C., Chen, W., et al. (2020). TCF-1 regulates the stem-like memory potential of HIV-specific CD8+ T cells in elite controllers. bioRxiv. https://doi.org/10.1101/2020.01.07.894535.

Sáez-Cirión, A., and Pancino, G. (2013). HIV controllers: a genetically determined or inducible phenotype? Immunol. Rev. *254*, 281–294.

Sáez-Cirión, A., Lacabaratz, C., Lambotte, O., Versmisse, P., Urrutia, A., Boufassa, F., Barré-Sinoussi, F., Delfraissy, J.F., Sinet, M., Pancino, G., and Venet, A.; Agence Nationale de Recherches sur le Sida EP36 HIV Controllers Study Group (2007). HIV controllers exhibit potent CD8 T cell capacity to suppress HIV infection *ex vivo* and peculiar cytotoxic T lymphocyte activation phenotype. Proc. Natl. Acad. Sci. USA *104*, 6776–6781.

Sáez-Cirión, A., Sinet, M., Shin, S.Y., Urrutia, A., Versmisse, P., Lacabaratz, C., Boufassa, F., Avettand-Fènoël, V., Rouzioux, C., Delfraissy, J.F., et al.; ANRS EP36 HIV Controllers Study Group (2009). Heterogeneity in HIV suppression by CD8 T cells from HIV controllers: association with Gag-specific CD8 T cell responses. J. Immunol. *182*, 7828–7837.

Sáez-Cirión, A., Shin, S.Y., Versmisse, P., Barré-Sinoussi, F., and Pancino, G. (2010). *Ex vivo* T cell-based HIV suppression assay to evaluate HIV-specific CD8+ T-cell responses. Nat. Protoc. *5*, 1033–1041.

Sáez-Cirión, A., Bacchus, C., Hocqueloux, L., Avettand-Fenoel, V., Girault, I., Lecuroux, C., Potard, V., Versmisse, P., Melard, A., Prazuck, T., et al.; ANRS VISCONTI Study Group (2013). Post-treatment HIV-1 controllers with a long-term virological remission after the interruption of early initiated antiretroviral therapy ANRS VISCONTI Study. PLoS Pathog. *9*, e1003211.

Santangelo, P.J., Rogers, K.A., Zurla, C., Blanchard, E.L., Gumber, S., Strait, K., Connor-Stroud, F., Schuster, D.M., Amancha, P.K., Hong, J.J., et al. (2015). Whole-body immunoPET reveals active SIV dynamics in viremic and antiretroviral therapy-treated macaques. Nat. Methods *12*, 427–432.

Schluns, K.S., Kieper, W.C., Jameson, S.C., and Lefrançois, L. (2000). Interleukin-7 mediates the homeostasis of naïve and memory CD8 T cells *in vivo*. Nat. Immunol. *1*, 426–432.

Simonetta, F., Hua, S., Lécuroux, C., Gérard, S., Boufassa, F., Sáez-Cirión, A., Pancino, G., Goujard, C., Lambotte, O., Venet, A., and Bourgeois, C. (2014). High eomesodermin expression among CD57+ CD8+ T cells identifies a CD8+ T cell subset associated with viral control during chronic human immunodeficiency virus infection. J. Virol. *88*, 11861–11871.

Snell, L.M., MacLeod, B.L., Law, J.C., Osokine, I., Elsaesser, H.J., Hezaveh, K., Dickson, R.J., Gavin, M.A., Guidos, C.J., McGaha, T.L., et al. (2018). CD8+ T Cell Priming in Established Chronic Viral Infection Preferentially Directs Differentiation of Memory-like Cells for Sustained Immunity. Immunity *49*, 678–694.

Sullivan, B.M., Juedes, A., Szabo, S.J., von Herrath, M., and Glimcher, L.H. (2003). Antigen-driven effector CD8 T cell function regulated by T-bet. Proc. Natl. Acad. Sci. USA *100*, 15818–15823.

Szabo, S.J., Sullivan, B.M., Stemmann, C., Satoskar, A.R., Sleckman, B.P., and Glimcher, L.H. (2002). Distinct effects of T-bet in TH1 lineage commitment and IFN-gamma production in CD4 and CD8 T cells. Science *295*, 338–342.

Takata, H., Buranapraditkun, S., Kessing, C., Fletcher, J.L., Muir, R., Tardif, V., Cartwright, P., Vandergeeten, C., Bakeman, W., Nichols, C.N., et al.; RV254/SEARCH010 and the RV304/SEARCH013 Study Groups (2017). Delayed differentiation of potent effector $CD8^+$ T cells reducing viremia and reservoir seeding in acute HIV infection. Sci. Transl. Med. *9*, eaag1809.

Takemoto, N., Intlekofer, A.M., Northrup, J.T., Wherry, E.J., and Reiner, S.L. (2006). Cutting Edge: IL-12 inversely regulates T-bet and eomesodermin expression during pathogen-induced CD8+ T cell differentiation. J. Immunol. *177*, 7515–7519.

Tansiri, Y., Rowland-Jones, S.L., Ananworanich, J., and Hansasuta, P. (2015). Clinical outcome of HIV viraemic controllers and noncontrollers with normal CD4 counts is exclusively determined by antigen-specific CD8+ T-cell-mediated HIV suppression. PLoS ONE *10*, e0118871.

Trautmann, L., Janbazian, L., Chomont, N., Said, E.A., Gimmig, S., Bessette, B., Boulassel, M.R., Delwart, E., Sepulveda, H., Balderas, R.S., et al. (2006). Upregulation of PD-1 expression on HIV-specific CD8+ T cells leads to reversible immune dysfunction. Nat. Med. *12*, 1198–1202.

Trautmann, L., Mbitikon-Kobo, F.M., Goulet, J.P., Peretz, Y., Shi, Y., Van Grevenynghe, J., Procopio, F.A., Boulassel, M.R., Routy, J.P., Chomont, N., et al. (2012). Profound metabolic, functional, and cytolytic differences characterize HIV-specific CD8 T cells in primary and chronic HIV infection. Blood *120*, 3466–3477.

Utzschneider, D.T., Charmoy, M., Chennupati, V., Pousse, L., Ferreira, D.P., Calderon-Copete, S., Danilo, M., Alfei, F., Hofmann, M., Wieland, D., et al. (2016). T Cell Factor 1-Expressing Memory-like CD8(+) T Cells

Sustain the Immune Response to Chronic Viral Infections. Immunity *45*, 415–427.

van den Berg, S.P.H., Pardieck, I.N., Lanfermeijer, J., Sauce, D., Klenerman, P., van Baarle, D., and Arens, R. (2019). The hallmarks of CMV-specific CD8 T-cell differentiation. Med. Microbiol. Immunol. (Berl.) *208*, 365–373.

Veazey, R.S., Gauduin, M.C., Mansfield, K.G., Tham, I.C., Altman, J.D., Lifson, J.D., Lackner, A.A., and Johnson, R.P. (2001). Emergence and kinetics of simian immunodeficiency virus-specific CD8(+) T cells in the intestines of macaques during primary infection. J. Virol. *75*, 10515–10519.

Walker, B., and McMichael, A. (2012). The T-cell response to HIV. Cold Spring Harb. Perspect. Med. *2*, a007054.

Ye, B., Liu, X., Li, X., Kong, H., Tian, L., and Chen, Y. (2015). T-cell exhaustion in chronic hepatitis B infection: current knowledge and clinical significance. Cell Death Dis. *6*, e1694.

Zhou, X., Yu, S., Zhao, D.M., Harty, J.T., Badovinac, V.P., and Xue, H.H. (2010). Differentiation and persistence of memory CD8(+) T cells depend on T cell factor 1. Immunity *33*, 229–240.

Zimmerli, S.C., Harari, A., Cellerai, C., Vallelian, F., Bart, P.A., and Pantaleo, G. (2005). HIV-1-specific IFN-gamma/IL-2-secreting CD8 T cells support CD4-independent proliferation of HIV-1-specific CD8 T cells. Proc. Natl. Acad. Sci. USA *102*, 7239–7244.

## STAR★METHODS

### KEY RESOURCES TABLE

| REAGENT or RESOURCE | SOURCE | IDENTIFIER |
|---|---|---|
| Antibodies | | |
| anti-CD3–PE (clone SP34-2) | BD Biosciences | Cat# 552127; RRID:AB_394342 |
| anti-CD3–AF700 (clone SP34-2) | BD Biosciences | Cat# 557917; RRID:AB_396938 |
| anti-CD4–PerCP-Cy5.5 (clone L200) | BD Biosciences | Cat# 552838; RRID:AB_394488 |
| anti-CD8–APC-Cy7 (clone RPA-T8) | BD Biosciences | Cat# 557760; RRID:AB_396865 |
| anti-CD8–BV650 (clone RPA-T8) | BioLegend | Cat# 301042; RRID:AB_2563505 |
| anti-CD14–BV786 (clone M5E2) | BD Biosciences | Cat# 563698; RRID:AB_2744287 |
| anti-CD20–BV786 (clone L27) | BD Biosciences | Cat# 740838; RRID:AB_2740492 |
| anti-CD27–PE (clone M-T271) | BD Biosciences | Cat# 555441; RRID:AB_395834 |
| anti-CD27–BUV395 (clone M-T271) | BD Biosciences | Cat# 740291; RRID: AB_2740030 |
| anti-CD28 (1 μg/mL, clone L293) | BD Biosciences | Cat# 340975; RRID:AB_400197 |
| anti-CD38–FITC (clone AT-1) | StemCell Technologies | Cat# 10415; RRID:AB_215564 |
| anti-CD45–V500 (clone D058-1283) | BD Biosciences | Cat# 561489; RRID:AB_10683313 |
| anti-CD45RA–PE-Cy7 (clone 5H9) | BD Biosciences | Cat# 561216; RRID:AB_10611721 |
| anti-CD49d (1 μg/mL, clone 9F10) | BD Biosciences | Cat# 555502; RRID:AB_395892 |
| anti-CD107a–V450 (clone H4A3) | BD Biosciences | Cat# 561345; RRID:AB_10646032 |
| anti-CD127–FITC (clone MB15-18C9) | Miltenyi Biotec | Cat# 130-113-410; RRID:AB_2733761 |
| anti-CCR5–APC (clone 3A9) | BD Biosciences | Cat# 560748; RRID:AB_1937308 |
| anti-CCR7–PE-Dazzle594 (clone G043H) | BioLegend | Cat# 353236; RRID:AB_2563641 |
| anti-CXCR5–BV710 (clone RF8B2) | BD Biosciences | Cat#740737; RRID:AB_2740408 |
| anti-HLA-DR–APC-H7 (clone G46-6) | BD Biosciences | Cat# 561358; RRID:AB_10611876 |
| anti-HLA-DR–Pacific Blue (clone G46-6) | BD Biosciences | Cat# 561359; RRID:AB_10645785 |
| anti-IFNγ–PE-Cy7 (clone B27) | BD Biosciences | Cat# 557643; RRID:AB_396760 |
| anti-IL-2–PE (clone MQ1-17H12) | BD Biosciences | Cat# 559334; RRID:AB_397231 |
| anti-Ki-67–AF700 (clone B56) | BD Biosciences | Cat# 561277; RRID:AB_10611571 |
| anti-T-bet–BV711 (clone 4B10) | BioLegend | Cat# 644820; RRID:AB_2715766 |
| anti-T*cf.*-1–PE (clone S33-966) | BD Biosciences | Cat# 564217; RRID:AB_2687845 |
| anti-TNFα–PE-CF594 (clone Mab11) | BD Biosciences | Cat# 562784; RRID:AB_2737791 |
| Bacterial and Virus Strains | | |
| SIVmac251 (uncloned) | A.M. Aubertin, Université Louis Pasteur, Strasbourg, France | N/A |
| Biological Samples | | |
| Blood and tissue samples from Mauritius Cynomolgus macaques | ANRS SIC Study | Approval local ethical committee: A13-005<br>Approval French Ministry of Education and Research: Number 44 |
| Blood samples from Mauritius Cynomolgus macaques | pVISCONTI study | Approval local ethical committee: A15-035<br>Approval French Ministry of Education and Research: Number 2453-2015102713323361v2 |
| Chemicals, Peptides, and Recombinant Proteins | | |
| Sodium Pentobarbital (Doléthal, Laboratoire Vetoquinol) | COVETO | Cat# 057327 |
| Ketamine chlorhydrate (Imalgene 1000®, Merial) | COVETO | Cat# 030901 |
| Emtricitabine (FTC) | Gilead Sciences | N/A |

(*Continued on next page*)

*Continued*

| REAGENT or RESOURCE | SOURCE | IDENTIFIER |
|---|---|---|
| Dolutegravir (DTG) | ViiV Healthcare | N/A |
| Tenofovir-disoproxil-fumarate (TDF) | Gilead Sciences | N/A |
| Ammonium chloride ($NH_4Cl$) | Sigma-Aldrich | Cat# 254134 |
| Potassium bicarbonate ($KHCO_3$) | Sigma-Aldrich | Cat# 60339 |
| EDTA 0,5 M UltraPure | Invitrogen | Cat# 15575020 |
| RPMI 1640 GlutaMAX | Life Technologies | Cat# 61870-010 |
| Fetal calf serum | Eurobio | Cat# CVFSVF00-01 |
| Penicillin-Streptomycin-Neomycin (PSN) Antibiotic Mixture | GIBCO | Cat# 15640055 |
| Penicillin-Streptomycin | GIBCO | Cat# 15140122 |
| Collagenase II | Sigma-Aldrich | Cat# C1764 |
| Percoll | Sigma-Aldrich | Cat# P1644 |
| Lymphocyte Separation Medium | Lonza Bioscience | Cat# 17-829E |
| Dulbecco's Phosphate Buffered Saline | Life Technologies | Cat# 14190144 |
| BD FACSLysing Solution 10X Concentrate | BD Biosciences | Cat# 349202 |
| BD Cytofix/Cytoperm Fixation/ Permeabilization Solution Kit | BD Biosciences | Cat# 554714 |
| Transcription Factor Buffer Set | BD Biosciences | Cat# 562574 |
| SIV peptides | ProImmune | Custom Order |
| SIVmac239 Gag Peptide Set | NIH AIDS Reagent Program | Cat# 12364 |
| BD GolgiStop™ Protein Transport Inhibitor | BD Biosciences | Cat# 554724 |
| Brefeldin A | Sigma-Aldrich | Cat# B7651-5MG |
| Concanavalin A from *Canavalia ensiformis* | Sigma-Aldrich | Cat# C5275 |
| Nef RM9 (RPKVPLRTM)–Mafa A1*063:02 | D. A. Price, Cardiff University, Cardiff, UK | N/A |
| Gag GW9 (GPRKPIKCW)–Mafa A1*063:02 | D. A. Price, Cardiff University, Cardiff, UK | N/A |
| Vpx GR9 (GEAFEWLNR)–Mafa B*095:01 | D. A. Price, Cardiff University, Cardiff, UK | N/A |
| Streptavidine APC eBioscience | Invitrogen | Cat# 17-4317-82 |
| Human IL-2 IS Premium grade | Miltenyi Biotec | Cat#130-097-748 |
| LIVE/DEAD® Fixable Aqua Dead Cell Stain Kit, for 405 nm excitation | Invitrogen | Cat# L34957 |
| Critical Commercial Assays | | |
| QIAamp DNA Blood Mini Kit | QIAGEN | Cat# 51106 |
| SuperScript III Platinum One-Step qRT-PCR | Invitrogen | Cat# 11732020 |
| CD14 MicroBeads, non-human primate | Miltenyi Biotec | Cat# 130-091-097 |
| EasySep Non-Human Primate CD4+ T Cell Isolation Kit | StemCell Technologies | Cat# 19582RF |
| EasySep Non-Human Primate Custom CD8+ Enrichment Kit | StemCell Technologies | Cat# 19809RF |
| ZeptoMetrix RETROtek SIV p27 Antigen ELISA Kit | Zeptometrix | Cat# 22-157-366 |
| Experimental Models: Cell Lines | | |
| SIV1C | F. Villinger. University of Louisiana, Lafayette, USA<br>Santangelo et al., 2015 | N/A |
| Oligonucleotides | | |
| SIV gag F: 5′-GCAGAGG AGGAAATTACCCAGTAC-3′ | Eurofins | Custom Order |
| SIV gag R: 5′-CAATTTTACC CAGGCATTTAATGTT-3′ | Eurofins | Custom Order |

(*Continued on next page*)

*Continued*

| REAGENT or RESOURCE | SOURCE | IDENTIFIER |
|---|---|---|
| SIV gag probe: 5′-FAM-TGTCCA CCTGCCATTAAGCCCGA-BHQ1-3′ | Eurofins | Custom Order |
| CCR5 F: 5′-CAACATGCTG GTCgATCCTCAT-3′ and 5′-CAAC ATACTGGTCGTCCTCATCC-3′ | Eurofins | Custom Order |
| CCR5 R: 5′-CAGCATAGT GAGCCCAGAAG-3′ | Eurofins | Custom Order |
| CCR5 probe: 5′-HEX-CTGACAT CTACCTGCTCAACCTG-BHQ1-3′ | Eurofins | Custom Order |
| Software and Algorithms | | |
| FlowJo software version 10 | TreeStar Inc. | https://www.flowjo.com |
| Tableau version 2018.1.4 | Tableau Software | https://www.tableau.com |
| GraphPad version 8.1.2 | Graphpad | https://www.graphpad.com |
| SigmaPlot version 12.5 | SYSTAT Software | http://www.sigmaplot.co.uk/products/sigmaplot/ |
| Other | | |
| gentleMACS Dissociator | Miltenyi Biotec | Cat# 130-093-235 |
| gentleMACS C Tubes | Miltenyi Biotec | Cat# 130-093-237 |
| HTS Transwell-96 system, reservoir and receiver plates with 2 lids, PC, 0.4μm | Corning | Cat# 3381 |

## RESOURCE AVAILABILITY

### Lead Contact

Further information and requests for resources and reagents should be directed to the Lead Contact, Asier Saez-Cirion (asier.saez-cirion@pasteur.fr). Request for biological resources will be fulfilled based on availability and upon the establishment of a MTA.

### Materials Availability

This study did not generate new unique reagents.

### Data and Code Availability

This study did not generate/analyze datasets/code.

## EXPERIMENTAL MODEL AND SUBJECT DETAILS

### Ethical statement

CyMs were imported from Mauritius and housed in facilities at the *Commissariat à l'Energie Atomique et aux Energies Alternatives* (CEA, Fontenay-aux-Roses, France). All non-human primate studies at the CEA are conducted in accordance with French National Regulations under the supervision of National Veterinary Inspectors (CEA Permit Number A 92-03-02). The CEA complies with the Standards for Human Care and Use of Laboratory Animals of the Office for Laboratory Animal Welfare under Assurance Number #A5826-01. All experimental procedures were conducted according to European Directive 2010/63 (Recommendation Number 9). The SIC and pVISCONTI studies were approved and accredited under statements A13-005 and A15-035 from the "*Comité d'Ethique en Expérimentation Animale du CEA*", registered and authorized under Number 44 and Number 2453-2015102713323361v2 by the French Ministry of Education and Research. CyMs were studied with veterinary guidance, housed in adjoining individual cages allowing social interactions, and maintained under controlled conditions with respect to humidity, temperature, and light (12 hr light/12 hr dark cycles). Water was available *ad libitum*. Animals were monitored and fed with commercial monkey chow and fruit once or twice daily by trained personnel. Environmental enrichment was provided in the form of toys, novel foodstuffs, and music under the supervision of the CEA Animal Welfare Body. Experimental procedures (animal handling, viral inoculations, and samplings) were conducted after sedation with ketamine chlorhydrate (Imalgene 1000®, 10 mg/kg, *i.v.*, Merial). Tissues were collected at necropsy. Animals were sedated with ketamine chlorhydrate and euthanized humanely with sodium pentobarbital (Doléthal, 180 mg/kg, *i.v.*, Laboratoire Vetoquinol).

### Animals and SIV infection

A total of 16 healthy adult male CyMs (median age = 6.8 years at inclusion, IQR = 5.8–7.2) were selected for this study on the basis of MHC haplotype ($M6^+$, n = 6; $M6^-$, n = 10) (Aarnink et al., 2011). CyMs were inoculated *i.r.* with either $5AID_{50}$ or $50AID_{50}$ of uncloned SIVmac251 (A.M. Aubertin, Université Louis Pasteur, Strasbourg, France). The following experimental groups were studied: (i) $M6^-$ CyMs inoculated *i.r.* with $5AID_{50}$ (non-M6 $5AID_{50}$, n = 4); (ii) $M6^+$ CyMs inoculated *i.r.* with $50AID_{50}$ (M6 $50AID_{50}$, n = 6); and (iii) $M6^-$ CyMs inoculated *i.r.* with $50AID_{50}$ (non-M6 $50AID_{50}$, n = 6). Animals were monitored for 18 months after infection.

The outcome of infection generally matched expectations based on previous studies for each experimental group (Figure S7A; Table S4). Only one $M6^+$ CyM (31041) was unable to control viremia below 400 copies/mL. This animal was homozygous for MHC class I (Table S1), which intrinsically limits immune control of HIV/SIV (Carrington et al., 1999; O'Connor et al., 2010). The dynamics of viral replication during acute infection were very similar in the three experimental groups, with peak VLs of 5.9, 6.4, and 6.3 log SIV-RNA copies/mL of plasma on day 14 *p.i.* for non-M6 $5AID_{50}$, M6 $50AID_{50}$, and non-M6 $50AID_{50}$ CyMs, respectively (Table S4).

CyMs in the pVISCONTI study (median age = 5 years at inclusion, IQR = 4.1–5.3) were inoculated *i.v.* with 1000 $AID_{50}$ of uncloned SIVmac251. None of these animals carried the M6 haplotype. An antiretroviral regimen containing emtricitabine (FTC, 40 mg/kg, Gilead), dolutegravir (DTG, 2.5 mg/kg, ViiV Healthcare), and the tenofovir prodrug tenofovir-disoproxil-fumarate (TDF, 5.1 mg/kg, Gilead), coformulated as a once daily subcutaneous injection, was initiated on day 28 *p.i.* in 6 animals.

## METHOD DETAILS

### Blood collection and processing

Peripheral blood was collected by venous puncture into Vacutainer Plus Plastic K3EDTA Tubes or Vacutainer CPT Mononuclear Cell Preparation Tubes with Sodium Heparin (BD Biosciences). Complete blood counts were monitored at all time points from the Vacutainer Plus Plastic K3EDTA Tubes. Plasma was isolated from Vacutainer Plus Plastic K3EDTA Tubes by centrifugation for 10 min at 1,500 g and stored at −80°C. Peripheral blood mononuclear cells (PBMCs) were isolated from Vacutainer CPT Mononuclear Cell Preparation Tubes with Sodium Heparin according to manufacturer's instructions (BD Biosciences), and red blood cells were lysed in ACK (0.15 M $NH_4Cl$, 10 mM $KHCO_3$, 0.1 mM EDTA, pH 7.4).

### Tissue collection and processing

Axillary or inguinal LNs (PLNs), RBs, and broncho-alveolar lavages (BALs) were collected longitudinally from each animal at the indicated time points. Bone marrow, spleen, mesenteric lymph nodes (MLNs), duodenum, jejunum, ileum, and colon were collected at necropsy. Tissue samples were snap-frozen in liquid nitrogen for storage at −80°C or collected in RPMI medium at 2–8°C. A complete PLN group was collected at each time point. LN cells were isolated into RPMI medium via mechanical disruption using a gentleMACS Dissociator (Miltenyi Biotec). The cell suspension was filtered (70 μm), and red blood cells were lysed in ACK. RB lymphocytes were obtained from approximately 4 $mm^2$ of rectal mucosa. Colonic lymphocytes were obtained from mucosa taken from approximately 10 cm of tissue. RBs and colonic tissue were washed extensively in R10 medium (RPMI medium supplemented with 10% fetal calf serum and penicillin/neomycin/streptomycin), and then digested for 45 min with collagenase II prior to mechanical disruption. Lymphocytes were isolated over a Percoll 67/44 gradient (Sigma-Aldrich). Bone marrow cells were purified using Lymphocyte Separation Medium (Lonza Bioscience) diluted to 90% in DPBS, centrifuged for 20 min at 350 g, and separated from red cells in ACK. Spleen cells were processed via mechanical disruption in RPMI medium using a gentleMACS Dissociator (Miltenyi Biotec), purified as described for bone marrow cells, and separated from red cells in ACK. T-cell activation and proliferation assays and measurements of SIV-suppressive activity were performed using freshly isolated cells, and intracellular cytokine assays and tetramer stains were performed using cells frozen viably at −80°C.

### Quantification of plasma viral load

Plasma viremia was monitored longitudinally in all animals using quantitative RT-PCR with a limit of detection of 12.3 copies/mL. Viral RNA was prepared from 100 μL of cell-free plasma. Quantitative RT-PCR was performed using a SuperScript III Platinum One-Step qRT-PCR Kit (Thermo Fisher Scientific) with a CFX96 Touch Real-Time PCR Detection System (Bio-Rad). Each tube contained 12.5 μL of 2X reaction mixture, 0.5 μL of RNaseOUT (40 U/μL), 0.5 μL of Superscript III Reverse Transcriptase/Platinum Taq DNA Polymerase, 1 μL of each primer (125 μM), 0.5 μL of the fluorogenic probe (135 μM), and 10 μL of eluted RNA. Primer/probe sequences were designed to amplify a region of SIVmac251 *gag*. The forward (F) primer sequence was 5′-GCAGAGGAGGAAAT TACCCAGTAC-3′ (24 bp), and the reverse (R) primer sequence was 5′-CAATTTTACCCAGGCATTTAATGTT-3′ (25 bp). The probe sequence was 5′-FAM-TGTCCACCTGCCATTAAGCCCGA-BHQ1-3′ (23 bp). This probe had a fluorescent reporter dye, FAM (6-carboxyfluorescein), attached to its 5′ end and a quencher, BHQ1 (Black Hole Quencher 1), attached to its 3′ end (TaqMan, Applied Biosystems). Samples were heated for 30 min at 56°C and 5 min at 95°C, followed by 50 thermocycles, each comprising 15 s at 95°C and 1 min at 60°C.

### Quantification of SIV-DNA

Total DNA was extracted from purified $CD14^+$ alveolar macrophages, buffy coats, and snap-frozen tissues. $CD14^+$ alveolar macrophages were purified magnetically via positive selection using CD14 MicroBeads (Miltenyi Biotec). Purity was checked using flow

cytometry (Figure S1B). Snap-frozen tissues were mechanically disrupted using a MagNA Lyser (Roche Diagnostics). DNA was extracted using a QIAamp DNA Blood Mini Kit (QIAGEN). SIV-DNA was quantified using an ultrasensitive quantitative real-time PCR. For blood samples, 150,000 cells were analyzed in each PCR. Sample limitations restricted input numbers to 20,000 cells for BALs and 50,000 cells for RBs. All amplifications were performed over 2–4 replicates. The cell line SIV1C, which contains 1 copy of SIV integrated/cell, was used as a standard for quantification. A total of 1 μg of DNA was considered to be equivalent to 150,000 cells. Amplification was performed using primers and a probe located in the *gag* region. The *CCR5* gene was used to normalize results per million cells. Results were adjusted by the frequencies of $CD4^+$ T cells in blood and tissues, according to availability. The limit of quantification was 2 copies/PCR. Primer and probe sequences were: SIV *gag* F: 5′-GCAGAGGAGGAAATTACCCAGTAC-3′; SIV *gag* R: 5′-CAATTTTACCCAGGCATTTAATGTT-3′; SIV *gag* probe: 5′-FAM-TGTCCACCTGCCATTAAGCCCGA-BHQ1-3′; *CCR5* F: an equimolar mix of 5′-CAACATGCTGGTCGATCCTCAT-3′ and 5′-CAACATACTGGTCGTCCTCATCC-3′; *CCR5* R: 5′-CAGCATAGT GAGCCCAGAAG-3′; and *CCR5* probe: 5′-HEX-CTGACATCTACCTGCTCAACCTG-BHQ1-3′.

### Viral reactivation in autologous $CD4^+$ T cells

Autologous $CD4^+$ T cells were purified magnetically from freshly isolated PBMCs using an EasySep CD4 Positive Selection Kit with an automated RoboSep (StemCell Technologies). Purified $CD4^+$ T cells were stimulated for 3 days with concanavalin A (5 μg/mL, Sigma-Aldrich) in the presence of IL-2 (100 IU/mL, Miltenyi Biotec). Stimulated $CD4^+$ T cells ($10^5$) were cultured in R10 medium containing IL-2 (100 IU/mL, Miltenyi Biotec). The production of SIV p27 was measured in culture supernatants on day 7 using an SIV p27 Antigen ELISA Kit (Zeptometrix).

### Measurement of T cell activation and proliferation

T cell activation and proliferation were assessed using fresh PBMCs and tissue cell suspensions. Blood samples were treated with FACS Lysing Solution (BD Biosciences). Cells were surface stained for CD3, CD4, CD8, CD38, CD45, CCR5, and HLA-DR, fixed/permeabilized using a Cytofix/CytoPerm Kit (BD Biosciences), and stained intracellularly for Ki-67. The following antibodies used were: anti-CD3–PE (clone SP34-2, BD Biosciences), anti-CD4–PerCP-Cy5.5 (clone L200, BD Biosciences), anti-CD8–BV650 (clone RPA-T8, BioLegend), anti-CD38–FITC (clone AT-1, StemCell Technologies), anti-CD45–V500 (clone D058-1283, BD Biosciences), anti-CCR5–APC (clone 3A9, BD Biosciences), anti-HLA-DR–APC-H7 (clone G46-6, BD Biosciences), and anti-Ki-67–AF700 (clone B56, BD Biosciences). Data were acquired using an LSRII flow cytometer (BD Biosciences) and analyzed with FlowJo software version 10 (Tree Star Inc.).

### Intracellular cytokine staining

Frozen PBMCs, PLN cells, bone marrow cells, splenocytes, and MLN cells were thawed, resuspended at $1 \times 10^6$/mL in R20 medium, and stored overnight at 37°C. Cells were then stimulated with a pool of 24 optimal SIV peptides (8–10 amino acids, 2 μg/mL each; Table S3) or with a pool of 125 overlapping SIV Gag 15-mer peptides (SIVmac239 Gag Peptide Set #12364, 2 μg/mL each, NIH AIDS Reagent Program) in the presence of anti-CD28 (1 μg/mL, clone L293, BD Biosciences) and anti-CD49d (1 μg/mL, clone 9F10, BD Biosciences) and stained with anti-CD107a (clone H4A3, BD Biosciences) for 30 min prior to the addition of GolgiStop (1 μL/mL, BD Biosciences) and brefeldin A (BFA, 5 μg/mL, Sigma-Aldrich). Costimulatory antibodies alone were used as a negative control, and concanavalin A (5 μg/mL, Sigma-Aldrich) was used as a positive control. Cells were incubated for a total of 6 hr. After washing, cells were surface stained for CD3, CD4, and CD8, fixed/permeabilized using a Cytofix/CytoPerm Kit (BD Biosciences), and stained intracellularly for IFNγ, TNFα, and IL-2. The following antibodies were used: anti-CD107a–V450 (clone H4A3, BD Biosciences), anti-CD3–AF700 (clone SP34-2, BD Biosciences), anti-CD4–PerCP-Cy5.5 (clone L200, BD Biosciences), anti-CD8–APC-Cy7 (clone RPA-T8, BD Biosciences), anti-IFNγ–PE-Cy7 (clone B27, BD Biosciences), anti-IL-2–PE (clone MQ1-17H12, BD Biosciences), and anti-TNFα–PE-CF594 (clone Mab11, BD Biosciences). Data were acquired using an LSRII flow cytometer (BD Biosciences) and analyzed with FlowJo software version 10 (Tree Star Inc.). Results were corrected for background by subtracting the negative (no peptide) control from the peptide stimulated response. Negative responses were given an arbitrary value of 0.001.

### MHC class I tetramer staining

Biotinylated complexes of Nef RM9 (RPKVPLRTM)–Mafa A1*063:02, Gag GW9 (GPRKPIKCW)–Mafa A1*063:02, and Vpx GR9 (GEAFEWLNR)–Mafa B*095:01 were produced as described previously (Price et al., 2005). The corresponding tetramers were generated via the stepwise addition of APC-conjugated streptavidin (Thermo Fisher Scientific). Frozen PBMCs were stained with all tetramers simultaneously for 30 min at 37°C, washed, and surface stained for CD3, CD4, CD8, CD14, CD20, CD27, CD45RA, CCR7, HLA-DR, and CD127. Cells were then fixed/permeabilized using a Cytofix/CytoPerm Kit (BD Biosciences) and stained for T-bet. The following antibodies were used: anti-CD3–AF700 (clone SP34-2, BD Biosciences), anti-CD4–PerCP-Cy5.5 (clone L200, BD Biosciences), anti-CD8–APC-Cy7 (clone RPA-T8, BD Biosciences), anti-CD14–BV786 (clone M5E2, BD Biosciences), anti-CD20–BV786 (clone L27, BD Biosciences), anti-CD27–PE (clone M-T271, BD Biosciences), anti-CD45RA–PE-Cy7 (clone 5H9, BD Biosciences), anti-CCR7–PE-Dazzle594 (clone G043H7, BioLegend), anti-HLA-DR–Pacific Blue (clone G46-6, BD Biosciences), anti-CD127–FITC (clone MB15-18C9, Miltenyi Biotec), and anti-T-bet–BV711 (clone 4B10, BioLegend). Data were acquired using an AriaIII flow cytometer (BD Biosciences) and analyzed with FlowJo software version 10 (Tree Star Inc.). MFI stands for median fluorescence intensity.

### TCF-1 staining

Frozen splenocytes were stained with tetramers as described above, washed, and surface stained for CD3, CD4, CD8, CD14, CD20, CD27, CD45RA, CCR7, and CXCR5. Cells were then fixed/permeabilized using a Transcription Factor Buffer Set (BD Biosciences) and stained for TCF-1. The following antibodies were used: anti-CD3–AF700 (clone SP34-2, BD Biosciences), anti-CD4–PerCP-Cy5.5 (clone L200, BD Biosciences), anti-CD8–APC-Cy7 (clone RPA-T8, BD Biosciences), anti-CD14–BV786 (clone M5E2, BD Biosciences), anti-CD20–BV786 (clone L27, BD Biosciences), anti-CD27–BUV395 (clone M-T271, BD Biosciences), anti-CD45RA–PE-Cy7 (clone 5H9, BD Biosciences), anti-CCR7–PE-Dazzle594 (clone G043H7, BioLegend), anti-CXCR5–BV710 (clone RF8B2, BD Biosciences), and anti-TCF-1–PE (clone S33-966, BD Biosciences). Data were acquired using an AriaIII flow cytometer (BD Biosciences) and analyzed with FlowJo software version 10 (Tree Star Inc.).

### Measurement of SIV-suppressive activity

Autologous $CD4^+$ and $CD8^+$ T cells were purified from freshly isolated PBMCs or tissue cell suspensions by positive and negative selection, respectively, using the relevant EasySep Kits with an automated RoboSep (StemCell Technologies). Purified $CD4^+$ T cells were stimulated for 3 days with concanavalin A (5 μg/mL, Sigma-Aldrich) in the presence of IL-2 (100 IU/mL, Miltenyi Biotec). Purified $CD8^+$ T cells were cultured in the absence of mitogens and cytokines (*ex vivo* $CD8^+$ T cells). Stimulated $CD4^+$ T cells ($10^5$) were superinfected in U-bottom 96-well plates with SIVmac251 (MOI = $10^{-3}$) in the presence (1:1 effector-to-target-cell ratio) or absence of *ex vivo* $CD8^+$ T cells ($10^5$) from the same tissue via spinoculation for 1 hr (1,200 g at room temperature) and incubated for 1 hr at 37°C. Purified $CD4^+$ and $CD8^+$ T cells were separated in some assays using HTS Transwell-96 Permeable Supports with 0.4-μm Pore Polycarbonate Membranes (Corning). Cells were then washed and cultured in R10 medium containing IL-2 (100 IU/mL, Miltenyi Biotec). Culture supernatants were assayed on day 7 using an SIV p27 Antigen ELISA Kit (Zeptometrix). Suppression of autologous virus was assessed similarly without superinfection. Antiviral activity was calculated as log10 (mean p27 ng/mL in SIV-infected $CD4^+$ T cell cultures without *ex vivo* $CD8^+$ T cells) / (mean p27 ng/mL in SIV-infected $CD4^+$ T cell cultures with *ex vivo* $CD8^+$ T cells) (Sáez-Cirión et al., 2010).

## QUANTIFICATION AND STATISTICAL ANALYSIS

Data visualization was performed using Tableau version 2018.1.4 (Tableau Software). Statistical analyses were performed using Prism version 8.1.2 (GraphPad Software) and SigmaPlot version 12.5 (SYSTAT Software). Results are presented as median ± IQR. Groups were compared using the Mann-Whitney U-test. Correlations were assessed using Spearman rank analyses. No adjustments were made for multiple comparisons, given the exploratory nature of the analyses. All p values less than 0.05 were defined as significant.